# Supporting information for Basic-to-acidic reversible pH switching with a merocyanine photoacid

Laura Wimberger,[a] Joakim Andréasson,[b] Jonathon E. Beves[a]
[a] School of Chemistry, UNSW Sydney, Sydney, New South Wales 2052, Australia
[b] Department of Chemistry and Chemical Engineering, Chalmers University of Technology, Göteborg 412 96, Sweden

# S1. General information

All data for this work is deposited on the ChemRxiv server, see Wimberger, L.; Andréasson, J.; Beves, J. *ChemRxiv* **2022**, DOI: 10.26434/chemrxiv-2022-wnts7. That content is a preprint and has not been peer-reviewed.

Reagents and solvents were purchased from Sigma-Aldrich, Chem Supply, BDH Chemicals or Combi-Blocks and used without further purification unless stated otherwise.
Qualitative TLC was performed on silica-coated aluminium plates (Merck, silica 60 F254) with detection by UV light ($\lambda$ = 254 nm). Flash column chromatography (FCC) was carried out with SilicaFlash® P60 (Velocity Scientific Solutions, 63 μm) with the indicated eluent.

**Nuclear magnetic resonance spectra** were recorded on a Bruker Avance III 300, Bruker Avance III 400 with a Prodigy CryoProbe, a Bruker Avance III 500 or a Bruker Avance III 600. Signals are reported relative to the residual $^{1}$H NMR signal of DMSO-$d_5$ ($\delta$ = 2.50 ppm) or $D_2O$ ($\delta$ = 4.79 ppm). $^{13}$C NMR spectra were referenced to the $^{13}$C-D septet of DMSO-$d_6$ ($\delta$ = 39.5). Coincidentally equal coupling constants of magnetically non-equivalent protons are marked as virtual (virt.). The signal multiplicities are indicated by the following abbreviations: s-singlet, d-doublet, t-triplet, q-quartet, quin-quintet, sex-sextet, sept-septet, m-multiplet, br-broad. The coupling constants *J* are reported in Hertz (Hz) as an average of the experimentally determined ones. Structural assignments are based on COSY, HMBC, and HSQC experiments.

**UV-vis absorption spectra** were measured in 41FLUV10 cells from fireflysci made of quartz (pathway 10 mm) on an Agilent Cary 60 UV-vis spectrometer equipped with a customized Cary Single Cell Peltier Accessory for temperature control (T = 22 °C) and stirring of the samples. A LED irradiation setup was employed as described previously by our group.[1] A Luxeon Rebel LED mounted ca. 4 cm away from the sample holder and focused with a Carclo 20.0 Fibre coupling lens served as irradiation source. Photoswitching cycles were controlled with a timer relay module (FRM01). For further details see S4.2.

**High resolution mass spectrometry** (HRMS) was measured on a hybrid linear quadrupole ion trap mass spectrometer (Thermo LTQ Orbitrap XL) with an external nanospray ionisation (NSI) source.

**pH values** were measured with a *Metrohm* 913 pH meter in conjunction with the *Metrohm* LL Biotrode 3mm WOC. The Pt1000 Temp Sensor Steel was used to monitor the temperature. Solutions in $D_2O$ were also measured with this pH meter and are reported as pD values.

# S2. Experimental procedures and analytical data

**Precursor synthesis**

4-(5-methoxy-2,3,3-trimethyl-3*H*-indol-1-ium-1-yl)butane-1-sulfonate

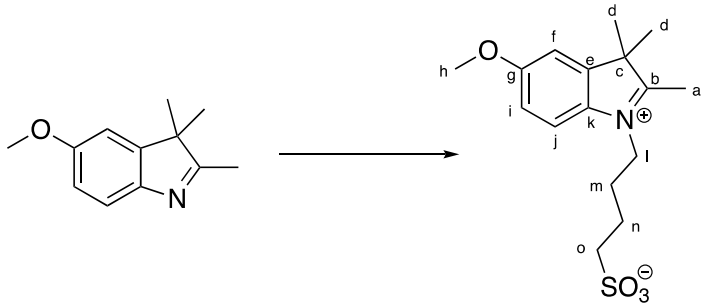


$C_{16}H_{23}NO_4S$
325.42 g/mol

5-Methoxy-2,3,3-trimethyl-3*H*-indole was prepared according to a literature procedure.[2] To a solution of propane 1,4-butane sultone (1.14 mL, 1.51 g, 1.05 eq.) in toluene anhydrous (8.6 mL), 5-methoxy-2,3,3-trimethyl-3*H*-indole (1.92 mL, 2.00 g, 1.00 eq.) was added under inert atmosphere and the solution was heated to 125 °C for 2.5 d. After letting it cool to r.t. the resulting solid was suspended in 8 mL of toluene. The dark purple solid was collected by vacuum filtration and washed with toluene (100 mL) and acetone (10 mL). The solid was dried *in vacuo* and resulted in 2.93 g of 4-(5-methoxy-2,3,3-trimethyl-3*H*-indol-1-ium-1-yl)butane-1-sulfonate (9.00 mmol, 85%) as dark purple solid and used without further purification in the consecutive reaction.

**$^1$H NMR** (600 MHz, DMSO-$d_6$): δ 7.92 (d, $J$ = 8.8 Hz, 1H, $H^j$), 7.46 (d, $J$ = 2.5 Hz, 1H, $H^f$), 7.13 (dd, $J$ = 8.8, 2.5 Hz, 1H, $H^i$), 4.46 – 4.41 (m, 2H, $H^l$), 3.85 (s, 3H, $H^h$), 2.78 (s, 3H, $H^a$), 2.49 (t, $J$ = 7.3 Hz, 2H, $H^o$), 1.98 – 1.90 (m, 2H, $H^m$), 1.71 (p, $J$ = 7.4 Hz, 2H, $H^n$), 1.50 (s, 6H, $H^d$).

**$^{13}$C NMR** (151 MHz, DMSO-$d_6$): δ 193.5 ($C^b$), 160.6 ($C^g$), 144.0 ($C^e$), 134.4 ($C^k$), 116.6 ($C^j$), 114.3 ($C^i$), 109.4 ($C^f$), 56.1 ($C^h$), 53.9 ($C^c$), 50.2 ($C^o$), 47.3 ($C^l$), 26.2 ($C^m$), 22.1 ($C^n$), 22.1 ($C^d$), 13.6 ($C^a$).

**HRMS** (ESI): calc. for $C_{16}H_{23}NO_4S$: $[M–H]^+$: 326.1421 $[M+Na]^+$:348.1240
found: $[M–H]^+$: 326.1423 $[M+Na]^+$: 348.1240.

$^1$H NMR (600 MHz, DMSO-$d_6$):

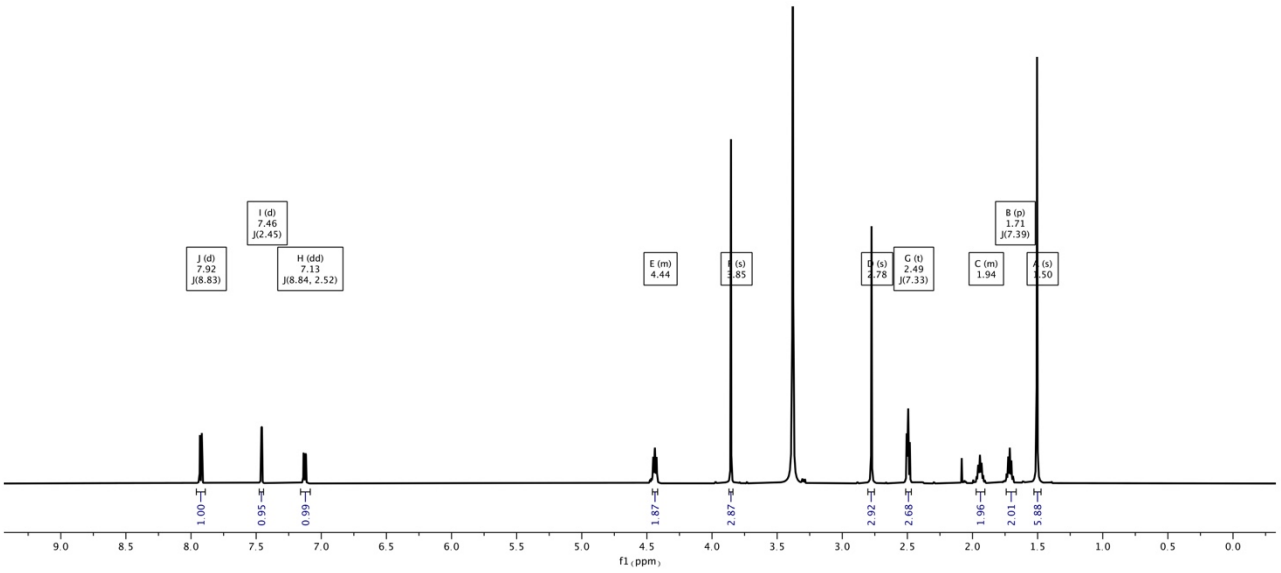

$^{13}$C NMR (151 MHz, DMSO-$d_6$):

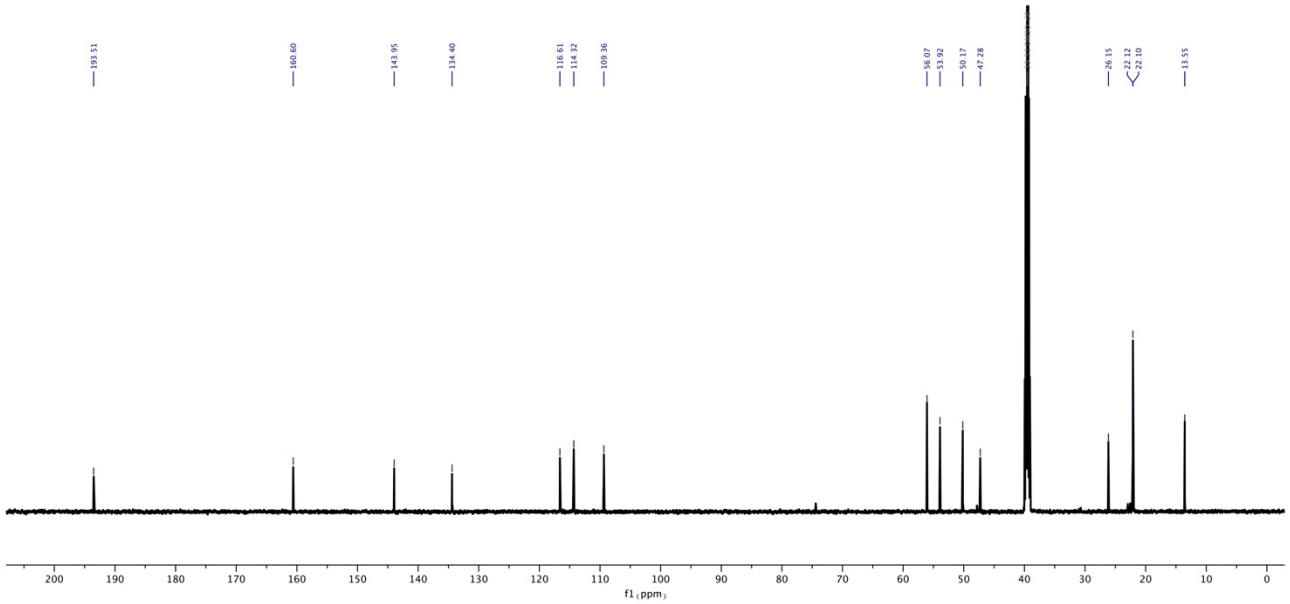


**Synthesis of SP-1/MCH-1**

(*E*)-4-(2-(2-hydroxystyryl)-5-methoxy-3,3-dimethyl-3*H*-indol-1-ium-1-yl)butane-1-sulfonate (**1**-MCH)/ (*R/S*)-4-(5'-methoxy-3',3'-dimethylspiro[chromene-2,2'-indolin]-1'-yl)butane-1-sulfonate (**1**-SP)

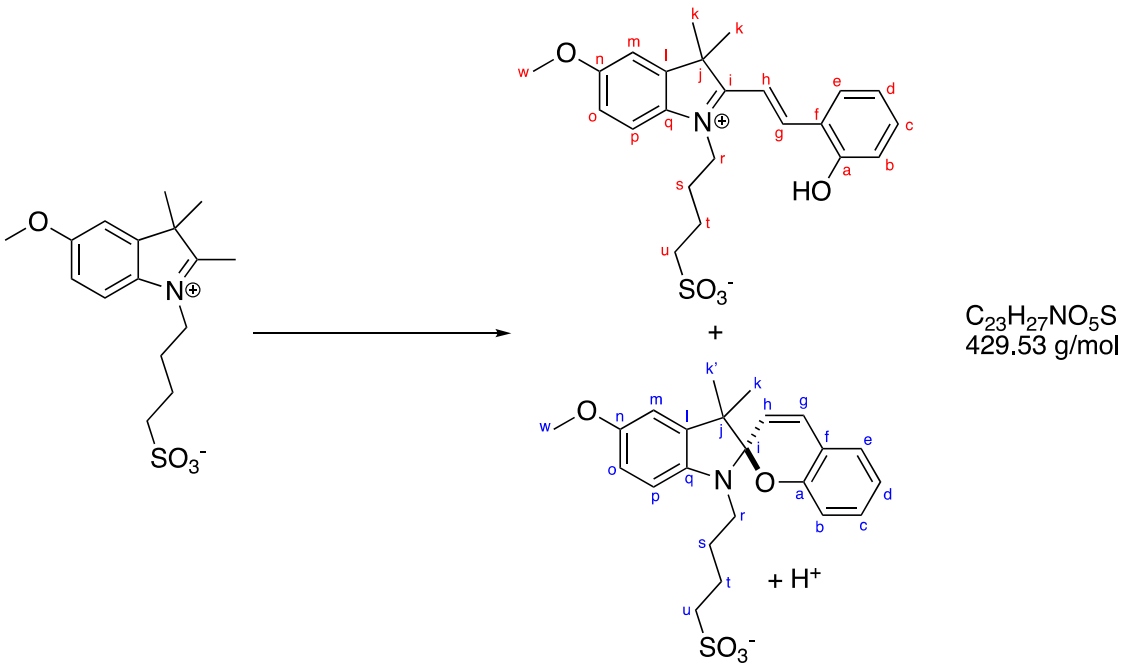


Salicylaldehyde (278 µL, 289 mg, 2.37 mmol, 1.10 eq., *BDH Chemicals*) was added to a solution of the substituted indolinium (700 mg, 2.15 mmol, 1.00 eq.) in anhydrous ethanol (0.27 M, 8.00 mL). The reaction mixture was heated to 100 °C for 19 h and cooled down to r.t. The reaction mixture was added dropwise to ice-cold diethyl ether (200 mL) resulting in an orange precipitate. The orange precipitate was collected by vacuum filtration and washed with ice cold diethyl ether (ca. 10 mL). The solid was purified by column chromatography (4.5 × 26 cm, $CH_2Cl_2$/MeOH = 95/5 → 93/7 → 90/10) resulting in an orange powder as the product (454 mg, 1.06 mmol, 49%). In solution (DMSO-$d_6$) **1** is present as a mixture of **MCH-1** and **SP-1**

**TLC**: $R_f$ = 0.38 ($CH_2Cl_2$/MeOH = 95/5) [UV].

***Merocyanine form***

**$^{1}$H NMR** (600 MHz, DMSO-$d_6$) δ 11.05 (s, 1H, OH), 8.46 (d, $J$ = 16.4 Hz, 1H, H$^{g}$), 8.15 (dd, $J$ = 8.0, 1.7 Hz, 1H, H$^{e}$), 7.91 (d, $J$ = 8.9 Hz, 1H, H$^{p}$), 7.74 (d, $J$ = 16.4 Hz, 1H, H$^{h}$), 7.51 (d, $J$ = 2.5 Hz, 1H, H$^{m}$), 7.44 (ddd, $J$ = 8.5, 7.1, 1.7 Hz, 1H, H$^{c}$), 7.15 (dd, $J$ = 8.9, 2.5 Hz, 1H, H$^{o}$), 7.03 (d, $J$ = 8.3 Hz, 1H, H$^{d/b}$), 7.00 – 6.97 (m, 1H, H$^{d/b}$), 4.59 (t, $J$ = 7.8 Hz, 2H, H$^{r}$), 3.89 (s, 3H, H$^{w}$), 2.54 – 2.51 (m, 2H, H$^{u}$), 1.96 (tt, $J$ = 8.2, 6.4 Hz, 2H. H$^{s}$), 1.82 – 1.77 (m, 2H, H$^{t}$), 1.76 (s, 6H, H$^{k}$).

**$^{13}$C{$^{1}$H} NMR** (151 MHz, DMSO-$d_6$) δ 179.5 (C$^{i}$), 160.8 (C$^{n}$), 158.8 (C$^{a}$), 147.2 (C$^{g}$), 145.7 (C$^{l}$), 135.1 (C$^{c}$), 134.2 (C$^{q}$), 130.2 (C$^{e}$), 121.4 (C$^{f}$), 119.9 (C$^{d/b}$), 116.6 (C$^{d/b}$), 116.4 (C$^{p}$), 114.9 (C$^{o}$), 111.8 (C$^{h}$), 108.8 (C$^{m}$), 56.2 (C$^{w}$), 51.9 (C$^{j}$), 50.3 (C$^{u}$), 46.6 (C$^{r}$), 27.1 (C$^{s}$), 26.4 (C$^{k}$), 22.3 (C$^{t}$).

***Spiropyran form***

**$^{1}$H NMR** (600 MHz, DMSO-$d_6$) δ 7.15 – 7.13 (m, 1H, H$^{e/c}$), 7.07 (td, $J$ = 7.7, 1.7 Hz, 1H, H$^{e/c}$), 6.96 (d, $J$ = 10.0 Hz, 1H, H$^{g}$), 6.80 (td, $J$ = 7.4, 1.1 Hz, 1H, H$^{d/b}$), 6.73 (d, $J$ = 2.6 Hz, 1H, H$^{m}$), 6.65 – 6.60 (m, 2H, H$^{o}$ ,H$^{d/b}$), 6.45 (d, $J$ = 8.4 Hz, 1H, H$^{p}$), 5.76 (d, $J$ = 10.2 Hz, 1H, H$^{h}$), 3.69 (s, 3H, H$^{w}$), 3.05 (dt, $J$ = 14.1, 7.0 Hz, 1H, H$^{r}$), 2.93 (dt, $J$ = 13.6, 5.8 Hz, 1H, H$^{r}$), 2.41 – 2.27 (m, 2H, H$^{u}$), 1.64 – 1.45 (m, 4H, H$^{s/t}$), 1.17 (s, 3H, H$^{k/k'}$), 1.08 (s, 3H, H$^{k/k'}$).

**$^{13}$C{$^{1}$H} NMR** (151 MHz, DMSO-$d_6$) δ 153.9 (C$^{a}$), 153.1 (C$^{n}$), 141.5 (C$^{q}$), 137.7 (C$^{l}$), 129.7 (C$^{e/c}$), 129.0 (C$^{g}$), 126.9 (C$^{e/c}$), 120.0 (C$^{d/b}$), 119.8 (C$^{h}$), 118.5 (C$^{f}$), 114.4 (C$^{d/b}$), 111.3 (C$^{o}$), 109.5 (C$^{m}$), 106.3 (C$^{p}$), 104.8 (C$^{i}$), 55.6 (C$^{w}$), 51.9 (C$^{j}$), 51.3 (C$^{u}$), 43.3 (C$^{r}$), 27.9 (C$^{s/t}$), 25.7 (C$^{k/k'}$), 22.8 (C$^{s/t}$), 19.7 (C$^{k/k'}$).

**HRMS** (ESI): calc. for $C_{23}H_{27}NO_5S$: $[M–Na]^+$: 452.1502
found: $[M–Na]^+$: 452.1502.

$^{1}$H NMR (600 MHz, DMSO-$d_6$):

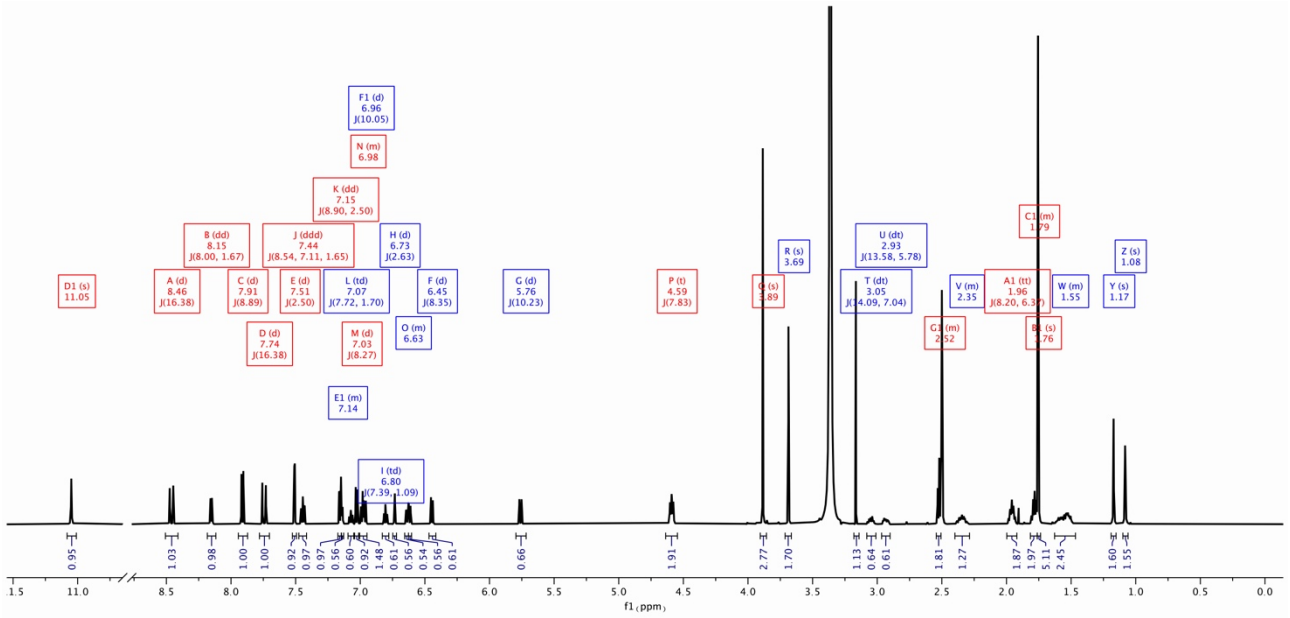

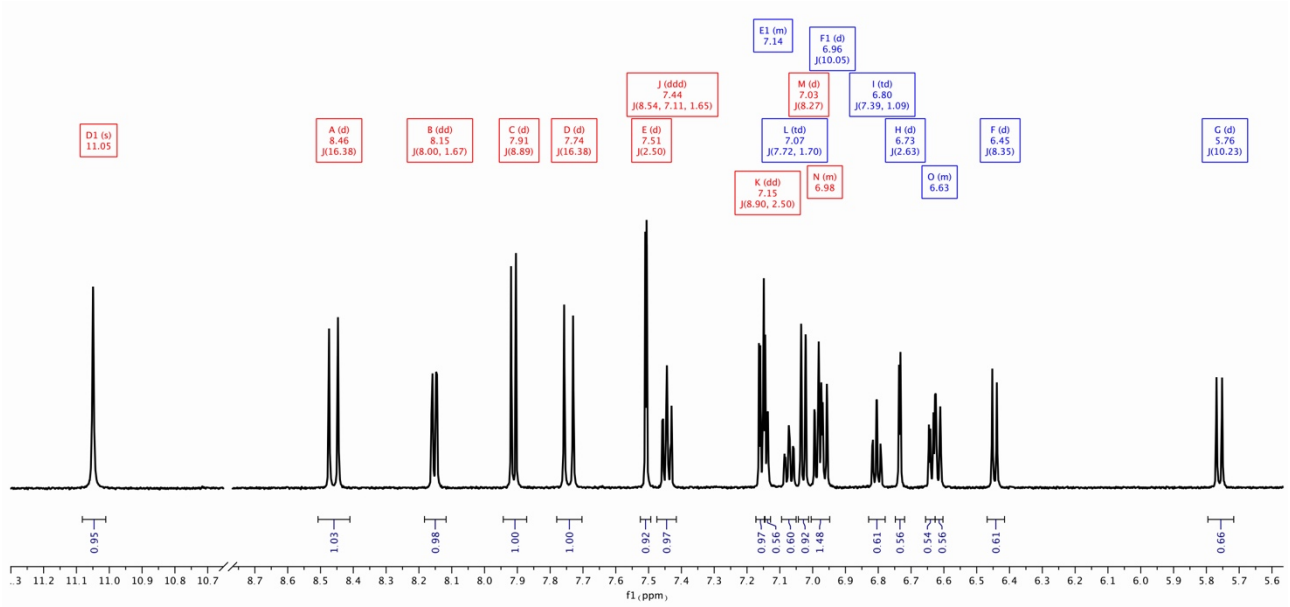


$^{13}$C NMR (151 MHz, DMSO-$d_6$):

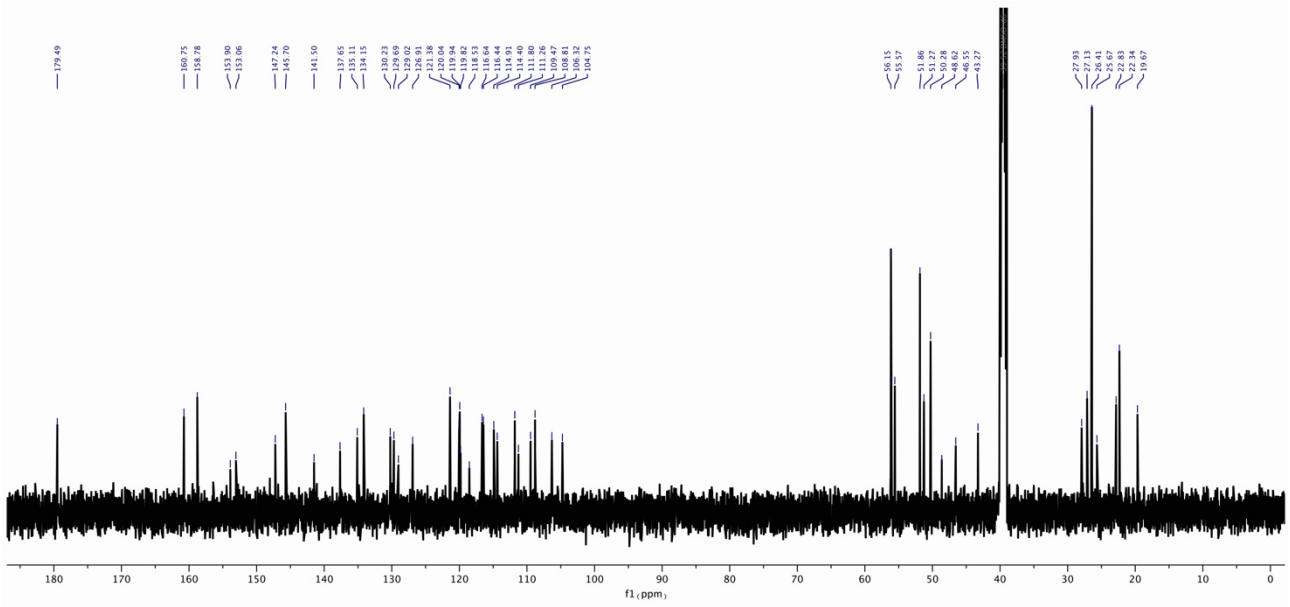

# S3. NMR studies

## S3.1. NMR titration of 1

Aqueous samples of **1** (1 mM) containing 10% $D_2O$ were prepared at different pH values with respective phosphate buffers (final phosphate concentration = 40 mM). At pH ~ 2 a mixture of the MCH form and *cis*-MCH form can be observed. The coupling constants of the alkene protons are characteristic for the individual species especially for the *cis*-MCH form which has previously been reported in the literature ($^3J_{cis}$ = 13.0 Hz)[3] and is in agreement with observed coupling constant of $^3J$ = 12.9 Hz. At pH ~ 5 predominantly the MCH form can be observed. At pH ~ 7 the concentration of MCH is lower, and small amounts of MC and SP are present. At the highest pH value (~ 9) the merocyanine form is predominantly deprotonated resulting in mostly the MC and SP forms.

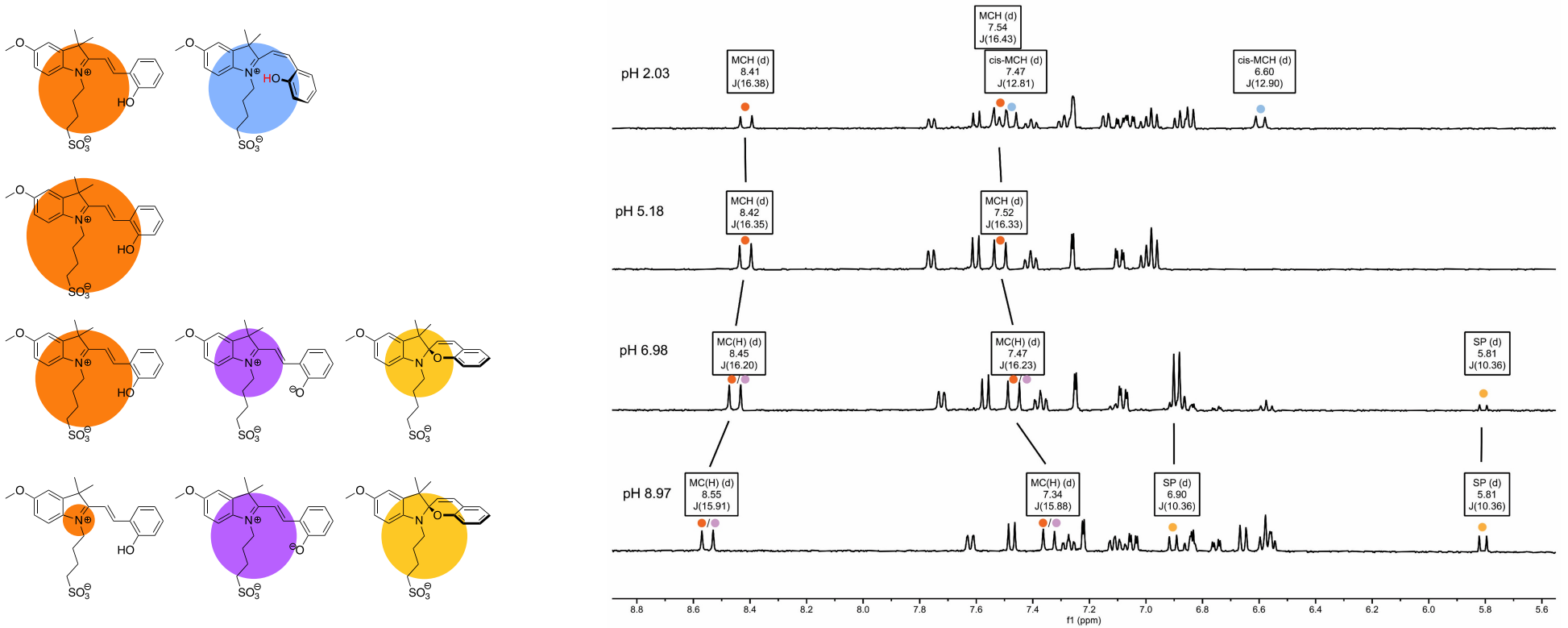


**Figure S1**. Representative distribution of species of **1** (left) for respective $^1$H NMR (400 MHz, 10% $D_2O$ in water, reduced power water suppression - zgcpgppr) spectra at varying pH values (right). The alkene doublets and coupling constants are characteristic for the respective species and are highlighted with respective colours (***cis*-MCH**, **MCH**, **MC**, **SP**).

Ratios of the individual species were determined by NMR by calculating the integral ratio of signals characteristic for the individual species: 6.60 ppm for *cis*-MCH, 8.41–8.55 for MC(H) and 5.81 ppm for SP. Additionally, ratios at respective pH values were calculated from p$K_a$ and $K_c$ values (determined by UV-vis absorbance titrations) following a reported method (see Eq. S1-3, ratios under light irradiation are calculated from Eq. S4-5).[2] The ratios calculated from UV-vis and NMR measurements at different pH values (see Table S1) are in good agreement which suggests that the parameters determined at micromolar concentrations from UV-vis absorbance studies are also applicable at higher concentrations (1 mM).

$$\chi_{MCH} = \frac{[MCH]}{C} = \frac{1}{(K_c + 1) \cdot 10^{pH - pK_a} + 1} \quad \text{(Eq. S1)}$$

$$\chi_{MC} = \frac{[MC]}{C} = \frac{1}{(K_c + 1) + \frac{1}{10^{pH - pK_a}}} \quad \text{(Eq. S2)}$$

$$\chi_{SP} = \frac{[SP]}{C} = \frac{K_c}{(K_c + 1) + \frac{1}{10^{pH - pK_a}}} \quad \text{(Eq. S3)}$$

$$\chi_{cis-MCH} = \frac{[cis\text{-MCH}]}{C} = \frac{1}{10^{pH - pK_a{}^{h\nu}} + 1} \quad \text{(Eq. S4)}$$

$$\chi_{SP_{h\nu}} = 1 - \chi_{cis\text{-MCH}} \quad \text{(Eq. S5)}$$

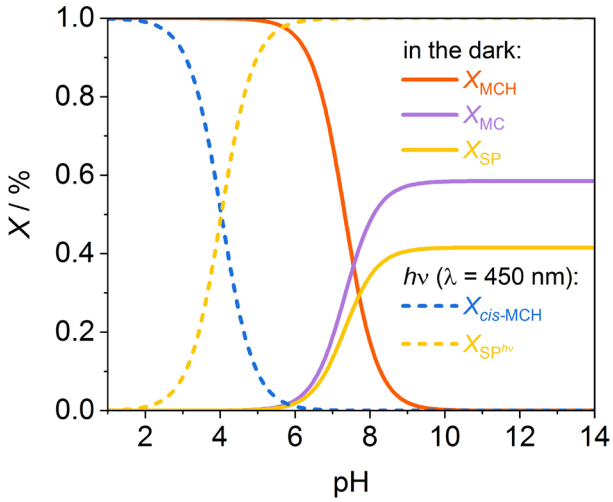


**Figure S2**. Overview of pH dependent mole fractions of MCH, MC, SP and *cis*-MCH calculated from Eq. S1-5.

**Table S1**. Comparison of ratios of individual species *cis*-MCH, MCH, MC and SP determined by NMR with ratios calculated from p$K_a$ and $K_c$ determined by UV-vis absorption.

| | Determined by NMR | | | | Calculated from parameters determined from UV-vis | | | |
|---|---|---|---|---|---|---|---|---|
| pH | *cis*-MCH | MCH | MC | SP | *cis*-MCH | MCH | MC | SP |
| 2.0 | 56 | 44 | – | – | – | – | – | – |
| 5.2 | – | 100 | | – | – | 99 | 0 | 0 |
| 7.0 | – | 89 | | 11 | – | 68 / 87 | 19 | 13 |
| 9.0 | – | 64 | | 36 | – | 2 / 58 | 57 | 41 |

## S3.2. Concentration dependent NMR of 1

Samples of increasing concentrations (0.8–3 mM) of **1** were prepared in $D_2O$. Increasing the concentration of **1** to approximately its solubility limit (3 mM) did not appear to result in aggregation of the MC(H) form. Since the equilibrium position of **1** is not significantly shifted towards the SP form we did not observe aggregation of the SP form as we did in an earlier study for concentrations above 1 mM.[2]

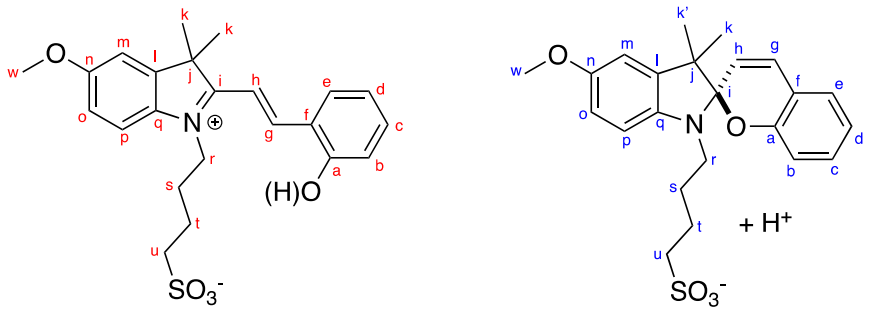


**1-MC(H)** **1-SP**

**Figure S3**. Structures of **1-MC(H)** and **1-SP** present at varying concentrations in the $^1$H NMR spectra shown below.

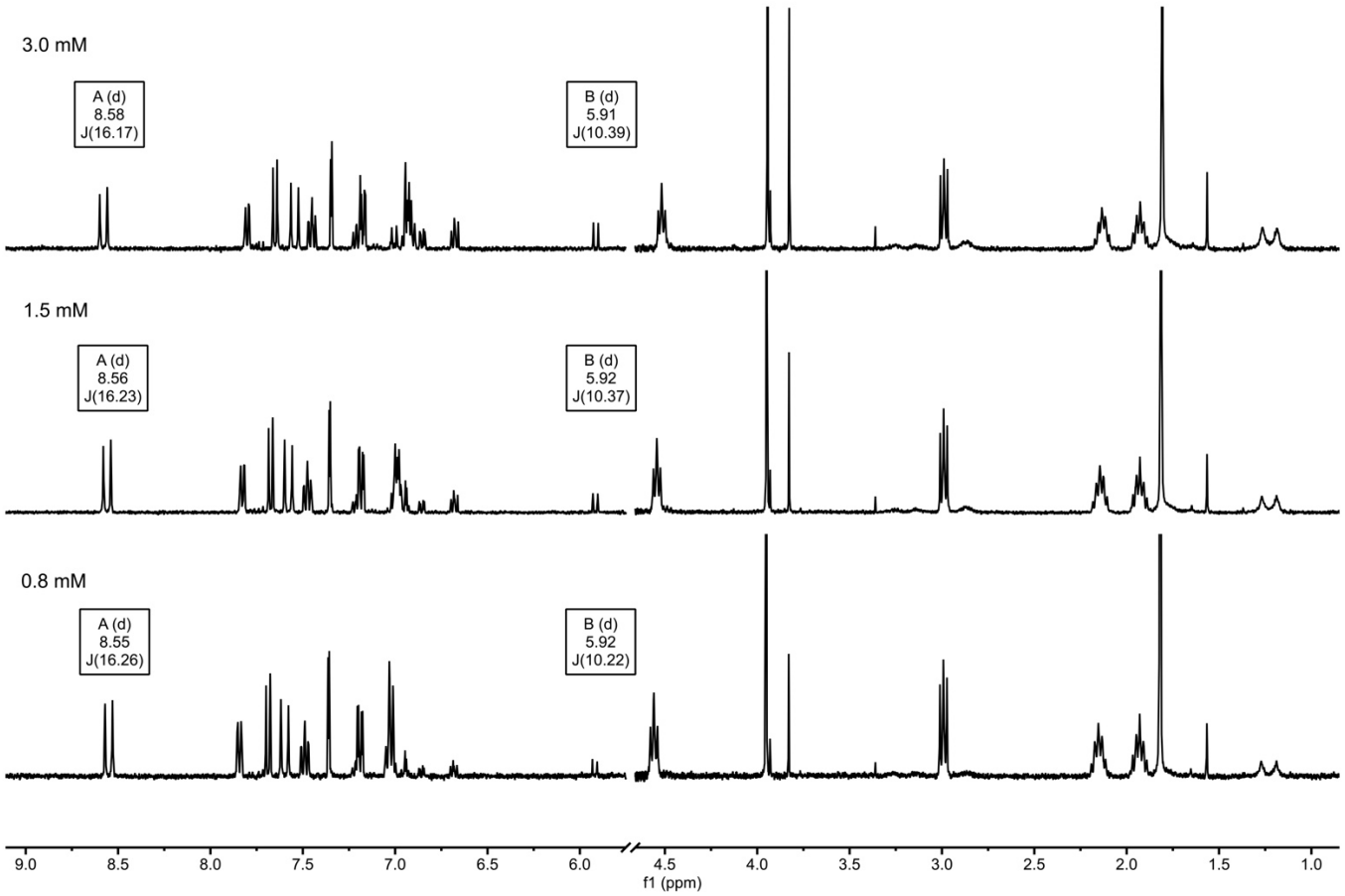


**Figure S4**. $^1$H NMR (400 MHz, $D_2O$) spectra of different concentrations of **1**. The doublet labelled as A corresponds to proton g of **1-MC(H)** and the doublet labelled as B corresponds to proton h of **1-SP**.

## S3.3. *In situ* irradiation $^1$H NMR spectra at increasing pD values

Solutions of **1** (1 mM) in $D_2O$ at increasing pD values were irradiated and monitored by $^1$H NMR spectroscopy. The NMR *in situ* irradiation setup[4] uses a fiber optic cable (Thorlabs, FT1500UMT) attached to a LUXEON Rebel color line LED light source (LXML-PR02-A900, Royal Blue) mounted to a heatsink. The fiber optic was fed into a screw cap NMR tube and inserted into the NMR spectrometer. The end of the fiber optic cable (ca. 3-4 cm) was roughened with sandpaper to ensure light emission across the entire sample volume. This setup allowed light irradiation during NMR acquisition.

The initial $^1$H NMR spectra in the dark at increasing pD values are shown below. The ratio of the MC(H) to SP form is calculated based on the characteristic alkene integrals (A: proton g of **1-MC(H)**, B: proton h of **1-SP**) which are highlighted in the NMR stack plot. As expected, the SP ratio increased with increasing pD values.

MC(H)/SP ratio / %

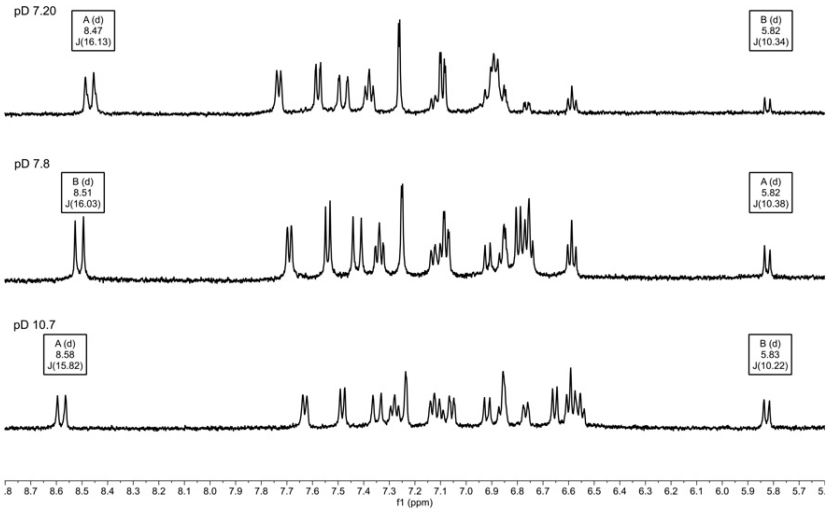


85 / 15

72 / 28

58 / 42

**Figure S5**. $^1$H NMR (500 MHz, $D_2O$) spectra in the dark at respective pD values with corresponding MC(H)/SP ratio determined from highlighted integrals (A: proton g of **1-MC(H)**, B: proton h of **1-SP**).

When irradiated with 455 nm light the doublet at 8.47–8.58 ppm characteristic for the MC(H) form disappears for samples below pD 8 which indicates a complete bleach. For the sample above pD 10 the integral of the doublet at 8.59 ppm corresponding to the MC(H) form is slightly decreased. This resulted in a larger SP ratio (51%) compared to in the dark (42%) which indicates that the sample is partly bleached.

MC(H)/SP ratio / %

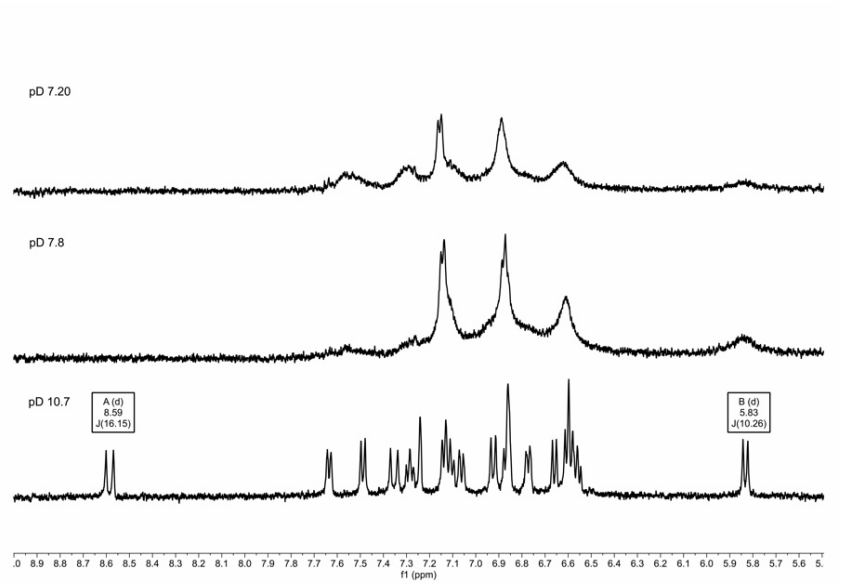


–

–

49 / 51

**Figure S6**. $^1$H NMR (500 MHz, $D_2O$) spectra under *hν* (λ = 455 nm) labelled according to initial pD values. The MC(H)/SP ratio was determined from highlighted integrals (A: proton g of **1-MC(H)**, B: proton h of **1-SP**).

After irradiation with 455 nm light all samples recovered back to their initial distribution in the dark (see below).

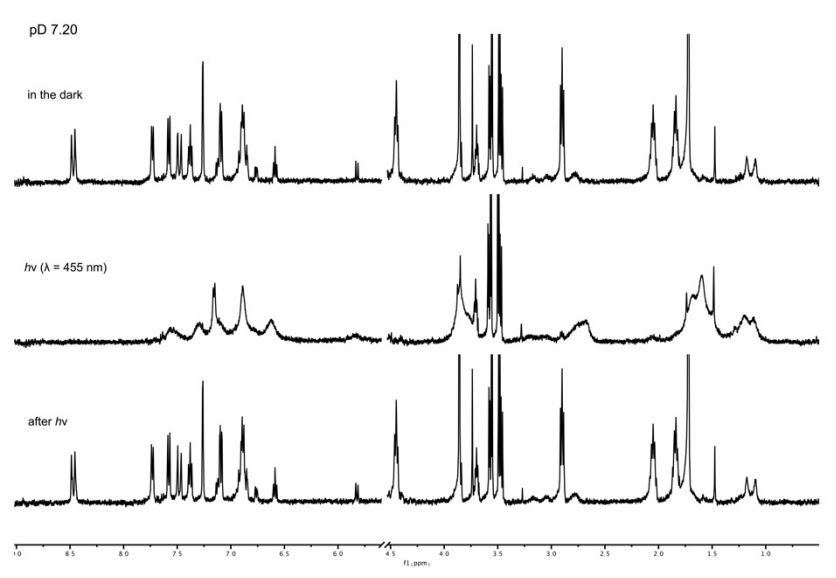


pD 7.2

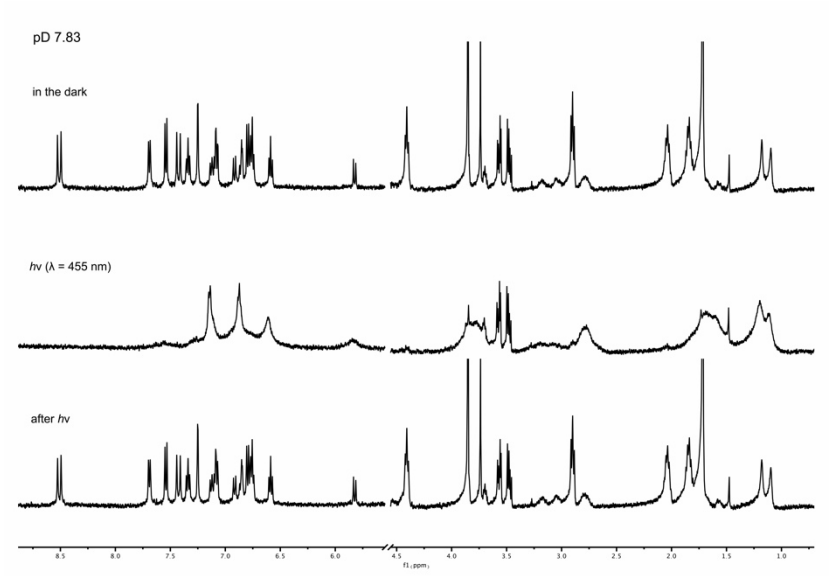


pD 7.8

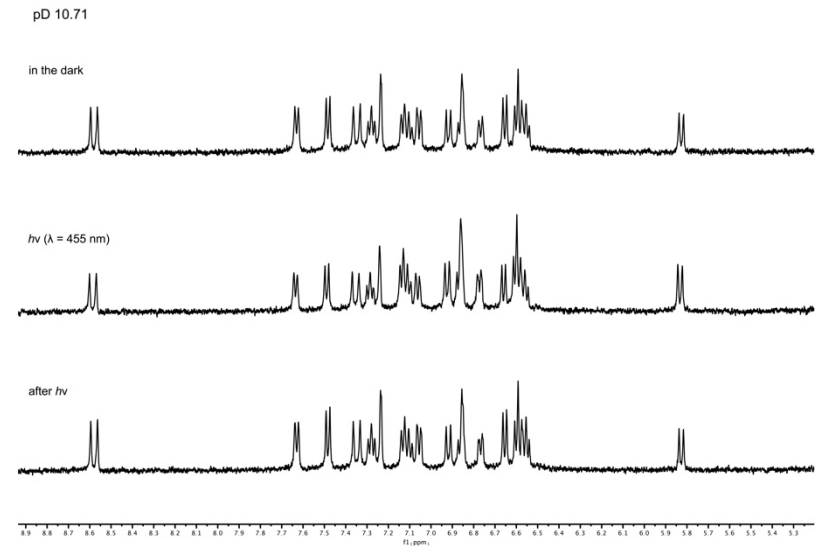


pD 10.7

**Figure S7**. $^{1}$H NMR (500 MHz, $D_2O$) spectra of **1** at increasing pD values (7.2-10.7). The respective top spectra were collected in the dark before irradiation, the middle spectra show the photo-stationary state under irradiation with 455 nm light, the bottom spectra show the fully recovered spectrum in the dark after irradiation.

The *in situ* irradiation in the NMR was monitored over time by collecting $^{1}$H NMR (500 MHz, $D_2O$) spectra every 31 seconds. Initially spectra were collected in the dark (2 min) followed by 5.2 min of irradiation at 455 nm and recovery in the dark after irradiation. Normalized integrals characteristic for the MC(H) (8.47–8.64 ppm) and SP (5.88–5.89 ppm) form were chosen to follow the bleaching process over time and are shown in Figure S8. For pD values 7.20 and 7.83 the samples appear to be fully bleached whereas at pD 10.7 no significant change is observed under light irradiation as indicated earlier (51% SP in the dark vs 42% SP under *h*ν).

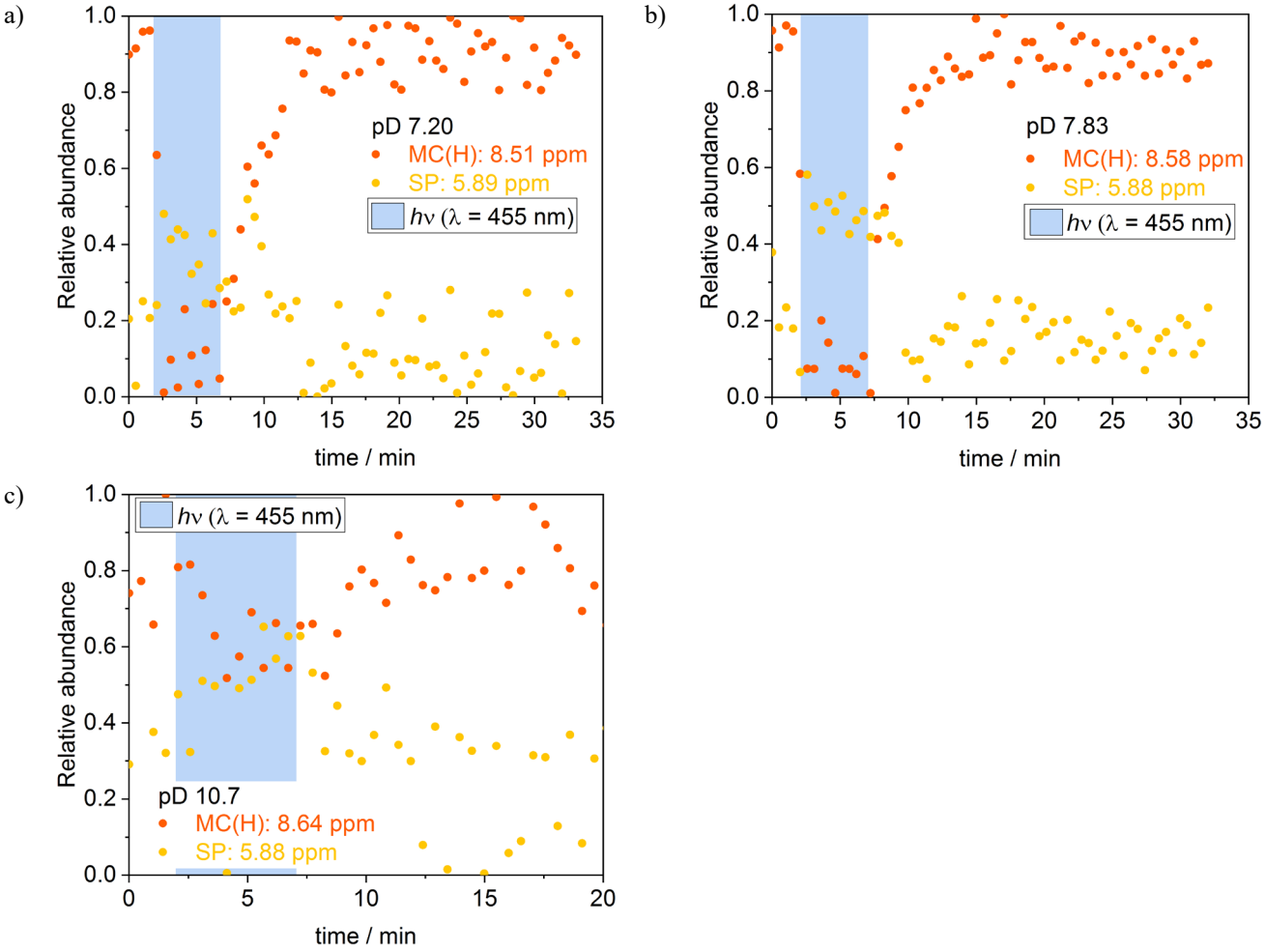


**Figure S8**. Kinetic traces following the *in situ* irradiation (λ = 455 nm, indicated by blue box) in the NMR at a) pD 7.20, b) pD 7.83 and c) pD 10.7. The respective normalized integrals characteristic for the MC(H) form at 8.5-8.6 ppm (orange) and the SP form at 5.9 ppm (yellow) are shown over time and were extracted from the respective $^{1}$H NMR spectra (500 MHz, $D_2O$).

# S4. UV-Vis studies

## S4.1. General procedure

Buffer solutions ranging from pH 2.5–10 were prepared by adding KOH (10 M) to $H_3PO_3$ (100 mM) solutions and pH 2.0–2.5 by adding standard HCl. The pH of the prepared solutions was measured with a *SPER* benchtop meter with a *ThermoFisher Scientific* Orion™ PerpHecT™ ROSS™ combination pH microelectrode.

A stock solution of **1** (c = 5.05 mM) was prepared with anhydrous methanol filtered through syringe filters (0.45 μm) and stored in a 10 mL volumetric flask wrapped in aluminum foil at 4 °C.

The stock solution was diluted with milliQ water to give 10% MeOH v/v (c ~500 μM).

**UV-vis samples preparation.** In a 1 cm cuvette 600 μL of a phosphate buffer of respective pH was mixed with 1800 μL of milliQ water, put in the spectrometer and let equilibrate thermally for 5 min. The acquisition was started and 450 μL of a premixed solution of milliQ water with 10% MeOH v/v dilution was added *in situ*, mixed by gentle pipetting and continuous stirring of the solution. Scans were collected until no further noticeable change in the spectrum occurred (20 min to ~3 h, pH dependent). The last spectrum of the scanning collection was used as the equilibrated spectrum in the dark.

For measurements of the *cis*-MCH and spiropyran forms, spectra were recorded under continuous irradiation (λ = 455 nm). For most pH values (except pH > 9) the equilibration was almost immediate and no change in the spectrum was observed over time. The last spectrum of the scanning collection under irradiation was used as the equilibrated spectrum in the light.

## S4.2. Setup for visible irradiation experiments (λ = 455 nm)

UV-Vis absorbance spectroscopy experiments were performed on an Agilent Cary 60 Bio UV-visible spectrophotometer equipped with a customized Cary Single Cell Peltier Accessory, maintaining the samples at a set temperature. The cell holder was modified to allow for irradiation perpendicular to the direction of measurement, as previously described.[4] A Luxeon Rebel LED was mounted on a heat sink positioned 4 cm away from the cell and driven using a 1000 mA LuxDrive PowerPuck. A Carclo 20.0 mm Fibre Coupling Lens was used to focus the beam. Samples were stirred to ensure homogeneity and a timer relay module (FRM01) was used to control the irradiation cycles.

**Table S2**. Technical information for LUXEON Rebel color line LED light source (https://www.lumileds.com/wp-content/uploads/files/DS68.pdf).

| LED part number | Descriptor maximum emission wavelength / nm | Dominant wavelength / nm | | Radiometric power / mW | | Test current / mA |
|---|---|---|---|---|---|---|
| | | Minimum | Maximum | Minimum | Typical | |
| LXML-PR02-A900 (Royal Blue) | 455 | 440 | 460 | 900 | 1030 | 700 |

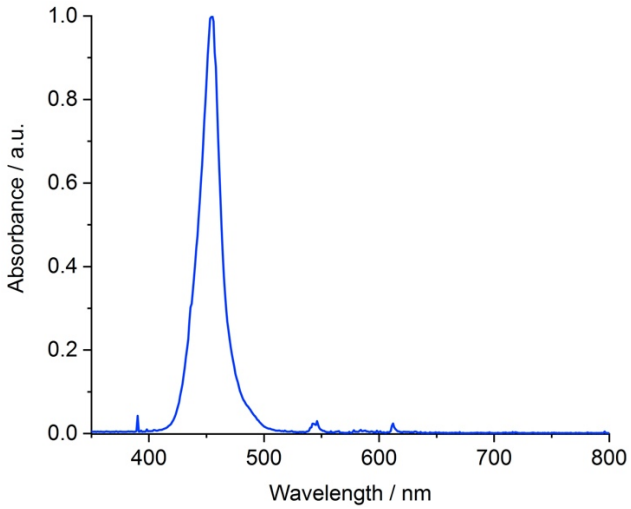


**Figure S9**. Emission spectrum of blue LED light source ($\lambda_{max}$ = 455 nm) for UV-vis irradiation experiments.

tas

## S4.3. p$K_a^{dark}$ and p$K_a^{hv}$ determination

The observed p$K_a$ values in the dark (p$K_a^{dark}$) and under irradiation (p$K_a^{hv}$) were determined using UV-vis spectroscopy based on previously reported methods.[2-3] Absorption spectra of equilibrated samples were recorded over the pH range in the dark and under irradiation with 455 nm light and are shown in Figure S10 a) and b). The characteristic absorbance maxima of the respective species were plotted over the pH range (Figure S10 c, d) and fitted to a sigmoidal function using origin:

$$A_{eq} = A_{OH} + \frac{A_H - A_{OH}}{1 + exp\left(\frac{pH - pK_a^{dark/hv}}{P}\right)} \quad \text{(Eq. S6)}$$

$A_{eq}$: absorbance at equilibrium

$A_{OH}$: absorbance at lowest recorded pH

$A_H$: absorbance at highest recorded pH

p$K_a^{dark/hv}$ approximate inflection point from plot

P = fitting factor

The reported p$K_a^{dark}$ and p$K_a^{hv}$ values are averaged and obtained from duplicate experiments. The reported errors are from standard deviation.

$pK_a^{dark} = 7.33 \pm 0.01$

$pK_a^{hv} = 4.03 \pm 0.03$

The previously defined photoacidity Π parameter was then calculated as:

$$\Pi = pK_a^{dark} - pK_a^{hv} = 3.29 \pm 0.03 \quad \text{(Eq. S7)}$$

a)

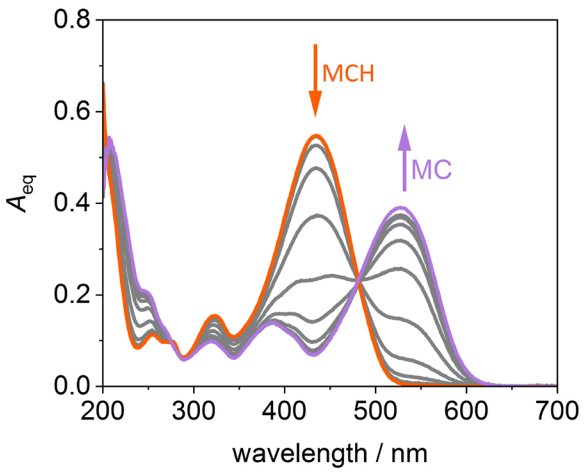


b)

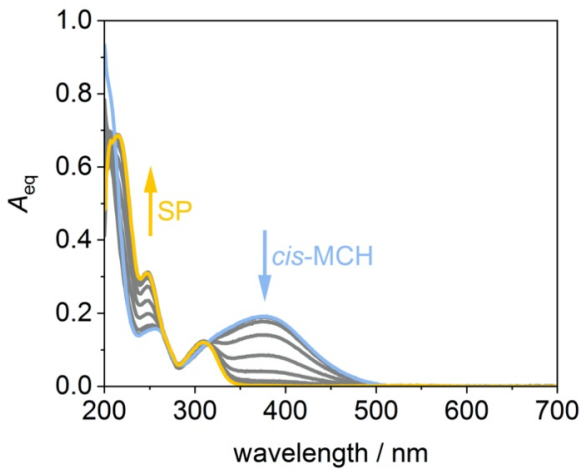

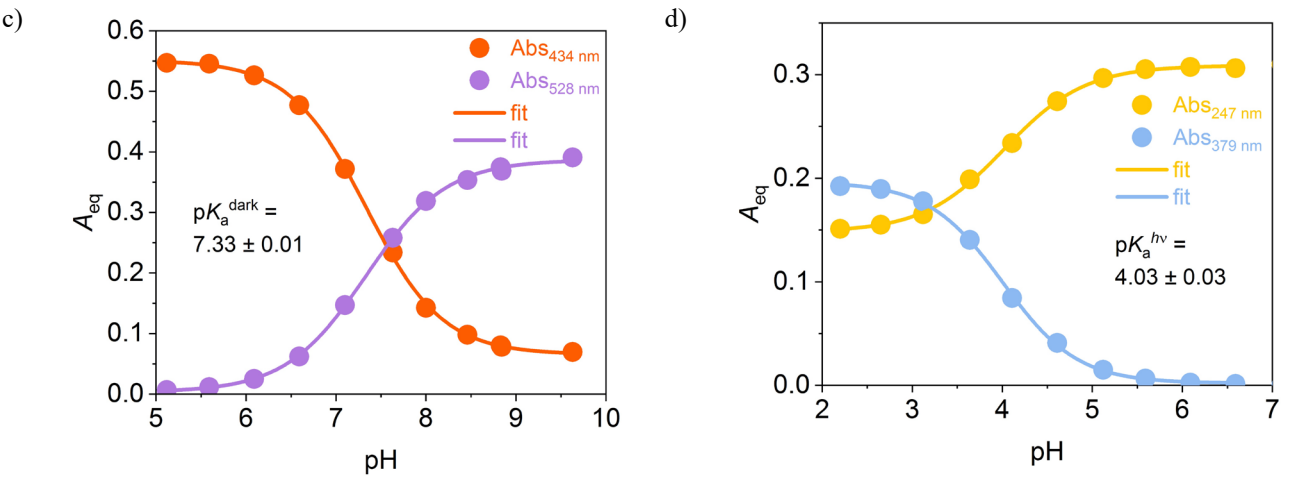


**Figure S10**. UV-vis absorption titrations of photoacid **1**. a) Equilibrated absorbance spectra at different pH values in the dark (orange: pH = 5.1, purple: pH = 9.6). b) Change in absorbance maxima of **1-MCH** (orange, λ = 434 nm) and **1-MC** (purple, λ = 528 nm) over the pH range with corresponding fits to Eq. S6 shown as solid lines. Experimental conditions: [**1**] = 20.0 µM, [phosphate buffer] = 20 mM, pH 5.1-9.6, $T$ = 22 °C. c) Equilibrated absorbance spectra at different pH values (blue: pH = 2.2, yellow: pH = 8.8) under continuous blue light irradiation (λ = 455 nm). d) Change in absorbance maxima of **1-SP** (yellow, λ = 247 nm) and **1-*cis*-MCH** (blue, λ = 379 nm) over the pH range with corresponding fits to Eq. S6 shown as solid lines. Experimental conditions: *hν* (λ = 455 nm), [**1**] = 20.0 µM, [phosphate buffer] = 20 mM, pH 2.2-8.8, $T$ = 22 °C.

## S4.4. Determination of kinetic parameters and p$K_a$

Kinetic parameters were determined by monitoring the equilibration process at varying pH values using UV-vis spectroscopy. The change of the maximum absorbance of the MCH form and MC form were monitored over time (Figure S11 a, b). These kinetic traces were fit to a single exponential function:

$$A_t = A_{eq} + (A_0 - A_{eq})e^{-k_{obs,eq}t} \quad \text{(Eq. S8)}$$

$A_t$: time dependent absorbance
$A_{eq}$: absorbance at equilibrium
$A_0$: absorbance at time = 0

The observed rate constants $k_{obs}$ are obtained from fitting the data to Eq. S8 and are averaged over duplicate experiments. Errors given are from standard deviation. The change of $k_{obs}$ over the pH range is shown in Figure S11 c). As reported previously[2-3] $k_{obs}$ is equal to the rate of ring opening $k_{open}$ where the pH value is < p$K_a^{dark}$ and > p$K_a^{hν}$. At pH >> p$K_a^{dark}$, the observed rate constant is equal to the sum of ring opening and ring closing rate constants ($k_{open}$ + $k_{close}$). The equilibrium constant $K_c$ can then be calculated as:

$$K_c = \frac{k_{close}}{k_{open}} \quad \text{(Eq. S9)}$$

Determined rate constants:

$k_{open} = 0.33 \pm 0.07 \times 10^{-2}$ s$^{-1}$ (pH 5.1)
$k_{close} + k_{open} = 0.57 \pm 0.11 \times 10^{-2}$ s$^{-1}$ (pH 8.9)
$k_{close} = 0.24 \pm 0.14 \times 10^{-2}$ s$^{-1}$
$K_c = 0.71 \pm 0.44$

The p$K_a$ can then be calculated using Eq. S10:[2]

$$K_a = \frac{K_a^{dark}}{(1 + K_c)} \quad \text{(Eq. S10)}$$

$$pK_a = pK_a^{dark} + \log(1 + K_c) \quad \text{(Eq. S11)}$$

p$K_a$ = 7.56 ± 0.11

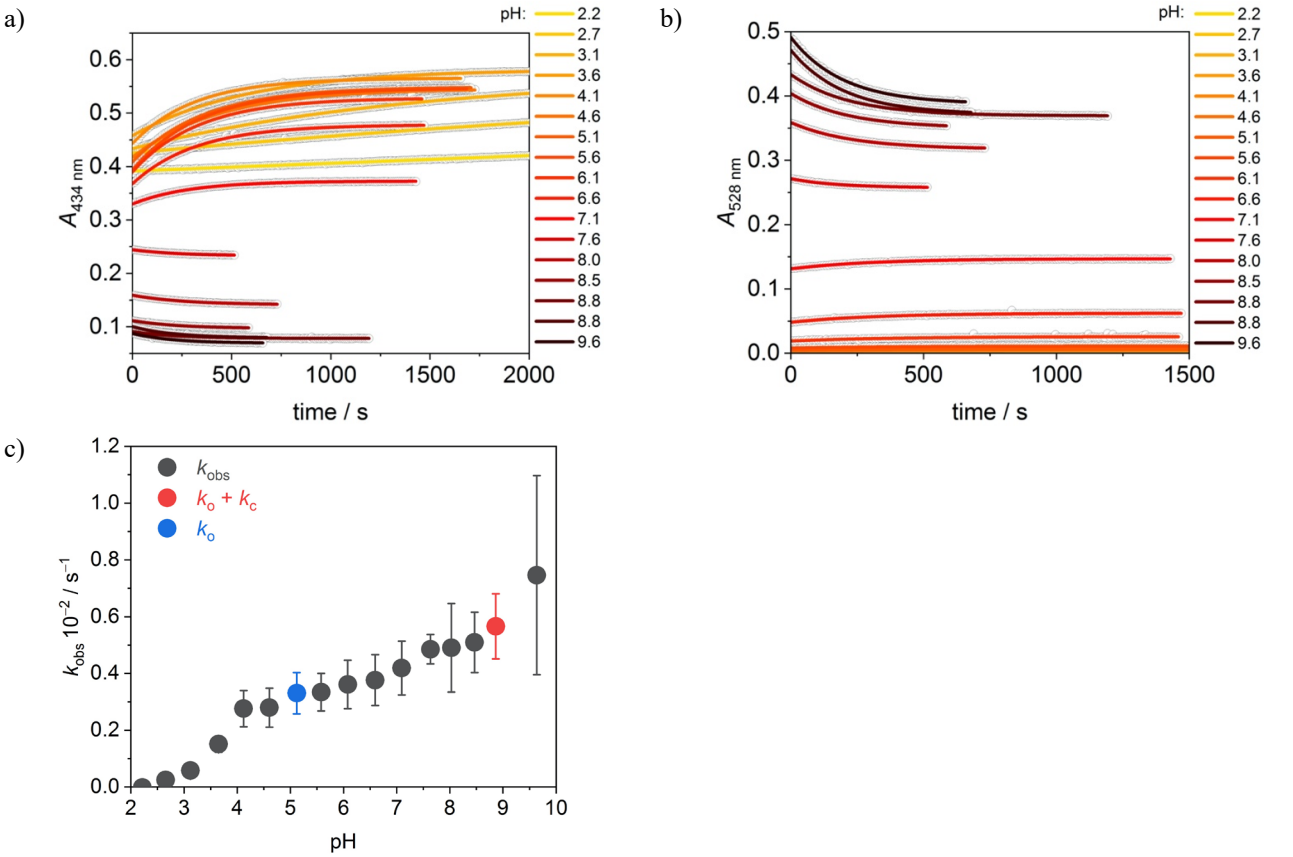


**Figure S11**. Kinetic parameters of photoacid **1**. An aqueous sample of the photoacid **1** was added to respective buffer solution *in situ* to monitor equilibration processes. a) Kinetic profiles for the equilibration of MCH (λ = 434 nm) at different pH (yellow = low pH, dark red = high pH) with corresponding exponential fits (Eq. S8) depicted as solid lines. Experimental conditions: [**1**] = 20.0 μM, [phosphate buffer] = 20 mM, pH 2.2-9.6, $T$ = 22 °C. b) Kinetic profiles for the equilibration of MC (λ = 528 nm) at different pH (yellow = low pH, dark red = high pH) with corresponding exponential fits (Eq. S8) depicted as solid lines. Experimental conditions: [**1**] = 20.0 μM, [phosphate buffer] = 20 mM, pH 2.2-9.6, $T$ = 22 °C. c) Averaged observed rate constants $k_{obs}$ from duplicate experiments obtained from the exponential fit to Eq. S8 in a) (error bars from standard deviation) with $k_o + k_c$ highlighted in red and $k_o$ highlighted in blue.

**Table S3**. $k_{obs}$ values from Figure S11 c) with respective half-lives ($t_{1/2} = \ln 2/k_{obs}$).

| pH | $k_{obs}\ 10^{-2}$ / $s^{-1}$ | $t_{1/2}$ / min |
|---|---|---|
| 2.22 | 0.00 ± 0.00 | – |
| 2.66 | 0.02 ± 0.01 | 46.3 |
| 3.12 | 0.06 ± 0.01 | 19.9 |
| 3.65 | 0.15 ± 0.03 | 7.7 |
| 4.12 | 0.28 ± 0.06 | 4.2 |
| 4.61 | 0.28 ± 0.07 | 4.1 |
| 5.12 | 0.33 ± 0.07 | 3.5 |
| 5.58 | 0.33 ± 0.07 | 3.5 |
| 6.08 | 0.36 ± 0.09 | 3.2 |
| 6.60 | 0.38 ± 0.09 | 3.1 |
| 7.10 | 0.42 ± 0.09 | 2.8 |
| 7.64 | 0.49 ± 0.05 | 2.4 |
| 8.03 | 0.49 ± 0.16 | 2.4 |
| 8.47 | 0.51 ± 0.11 | 2.3 |
| 8.87 | 0.57 ± 0.11 | 2.0 |
| 9.64 | 0.75 ± 0.35 | 1.5 |

## S4.5. Extinction coefficients

By choosing specific experimental conditions pure absorbance spectra of the SP and MCH form could be obtained. Experimental conditions are given below Figure S12. At high pH an absorbance spectrum of a mixture of the SP and MC was obtained and used to calculate the extinction coefficients of the MC form ($\varepsilon_{MC,\lambda}$) using Eq. S12:[3]

$$\varepsilon_{MC,\lambda} = \frac{A_{eq} - \varepsilon_{SP,\lambda}\chi_{SP}C}{\chi_{MC}C} \qquad \text{(Eq. S12)}$$

$A_{eq}$: absorbance at equilibrium

$\varepsilon_{SP,\lambda}$: extinction coefficient of the SP form

$\chi_{SP}$: mole fraction of the SP form

$\chi_{MC}$: mole fraction of the MC form

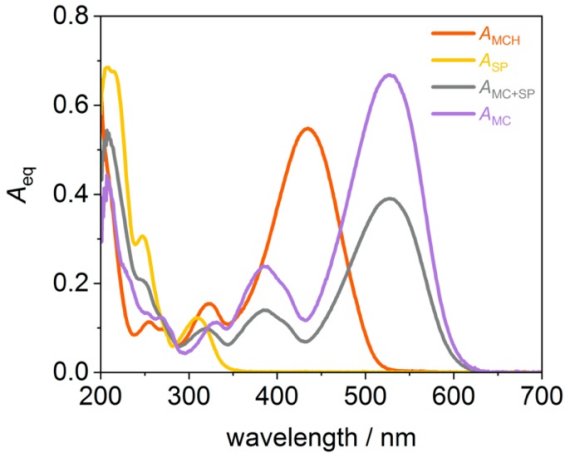


**Figure S12**. Absorbance spectra of SP (yellow), MCH (orange), an equilibrated absorbance spectrum at high pH containing SP and MC (grey) used to calculate spectrum of MC (purple) with Eq. S13. Experimental conditions: [**1**] = 20.0 µM, [phosphate buffer] = 20 mM, $T$ = 22 °C.

| $A_{SP}$ under $h\nu$ ($\lambda$ = 455 nm) | $A_{MCH}$ (dark) | $A_{SP+MC}$ (dark) | $A_{MC}$[3] |
|---|---|---|---|
| pH 6.6 | pH 5.1 | pH 9.6 | $A^{\lambda}_{MC} = \frac{A^{\lambda}_{eq} - A^{\lambda}_{SP}\chi_{SP}}{\chi_{MC}}$ where $A^{\lambda}_{SP} = \varepsilon^{\lambda}_{SP}C$ (Eq. S13) |

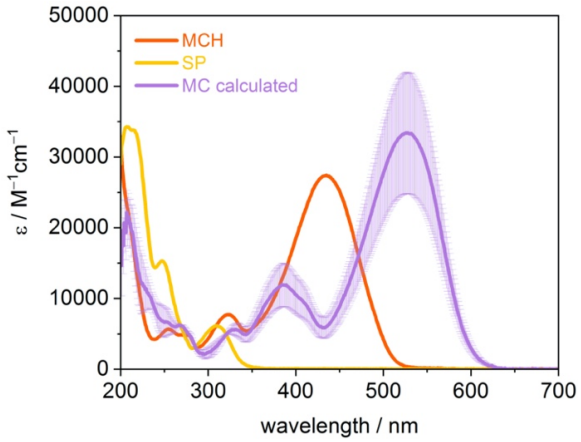


**Figure S13**. Extinction coefficients of the respective species showing error bars ($\delta\varepsilon_{MC,\lambda_{max}}$) for the calculated MC extinction coefficients (Eq. S12) which were determined by error propagation: Errors of $A_{eq}, \varepsilon_{SP,\lambda_{max}}, C$ assumed to be negligible compared to the error from $K_c$:

$$\delta\varepsilon_{MC,\lambda_{max}} = \sqrt{\left(\frac{\partial\varepsilon_{MC,\lambda_{max}}}{\partial K_c}\right)^2 (\delta K_c)^2} = \sqrt{\left(\frac{A_{eq}}{C} - \varepsilon_{SP,\lambda_{max}}\right)^2 (\delta K_c)^2}$$

**Table S4**. Overview of extinction coefficients of the SP, MCH and MC form at selected absorbance maxima characteristic for the individual species

| $\lambda$ /nm | $\varepsilon_{SP}$ / $10^3 \times$ L mol$^{-1}$cm$^{-1}$ | $\varepsilon_{MCH}$ / $10^3 \times$ L mol$^{-1}$cm$^{-1}$ | $\varepsilon_{MC}$ / $10^3 \times$ L mol$^{-1}$cm$^{-1}$ |
|---|---|---|---|
| 247 | 15.3 | 5.0 | 6.8 ± 2.2 |
| 434 | – | 27.4 | 5.9 ±1.5 |
| 528 | – | – | 33.4 ± 8.6 |

# S5. pH switching

Concentrated solutions of **1** (2-3 mM) were prepared in 20 mM aqueous KCl solution. Less concentrated samples were prepared by diluting the concentrated solution by a factor of 10.

## S5.1. Penn PhD photoreactor

The sample was irradiated in a *Penn PhD* photoreactor m2 with 10 s of pre-stirring, 30–60 s of irradiation with 450 nm light at full power followed by stirring in the dark. The cooling fan was set to its maximum capacity. Using the internal temperature control of the photoreactor in combination with a photocoupler resulted in larger temperature spikes under irradiation compared to setting the fan to full speed.

**pH switching at different initial pH values**

The pH value was adjusted by adding 0.7–2 µL of aqueous KOH (1 M) to 3.2 mL of a solution of **1** and letting the sample equilibrate for a minimum of five half-lives (changes depending on the pH). The corresponding amounts of base added resulting in $pH_{initial}$ values and the pH values reached under irradiation are shown in Table S5-6.

**Table S5**. pH adjustments of a concentrated solution of **1** (2.4 mM) and respective light induced pH changes.

| # | V of 1 M KOH added / µL | Sum of equivalents of KOH added | $pH_{initial}$ | $pH_{h\nu}$ | ΔpH |
|---|---|---|---|---|---|
| 1 | – | – | 7.24 | 3.74 | 3.50 |
| 2 | 0.7 | 0.0002 | 7.33 | 3.85 | 3.48 |
| 3 | 1.5 | 0.0007 | 7.48 | 4.04 | 3.44 |
| 4 | 1.5 | 0.0012 | 7.55 | 4.20 | 3.35 |
| 5 | 2.0 | 0.0019 | 7.82 | 4.59 | 3.23 |
| 6 | 2.0 | 0.0026 | 8.31 | 5.74 | 2.57 |
| 7 | 1.0 | 0.0029 | 8.67 | 7.78 | 0.89 |

**Table S6**. pH adjustments of a diluted solution of **1** (0.21 mM) and respective light induced pH changes.

| # | V of 0.1 M KOH added / µL | Sum of equivalents of KOH added | $pH_{initial}$ | $pH_{h\nu}$ | ΔpH |
|---|---|---|---|---|---|
| 1 | – | – | 7.00 | 4.29 | 2.71 |
| 2 | 0.7 | 0.0002 | 7.12 | 4.41 | 2.71 |
| 3 | 1.5 | 0.0007 | 7.27 | 4.67 | 2.60 |
| 4 | 1.5 | 0.0012 | 7.41 | 5.01 | 2.40 |
| 5 | 2.0 | 0.0019 | 7.56 | 5.74 | 1.82 |
| 6 | 2.0 | 0.0026 | 7.75 | 6.37 | 1.38 |
| 7 | 1.0 | 0.0029 | 7.78 | 6.56 | 1.22 |
| 8 | 2.0 | 0.0036 | 7.92 | 6.98 | 0.94 |
| 9 | 2.0 | 0.0042 | 8.14 | 7.62 | 0.52 |

The change in pH and temperature over time of experiments listed in Tables S5-6 are shown in Figure S14.

2.4 mM

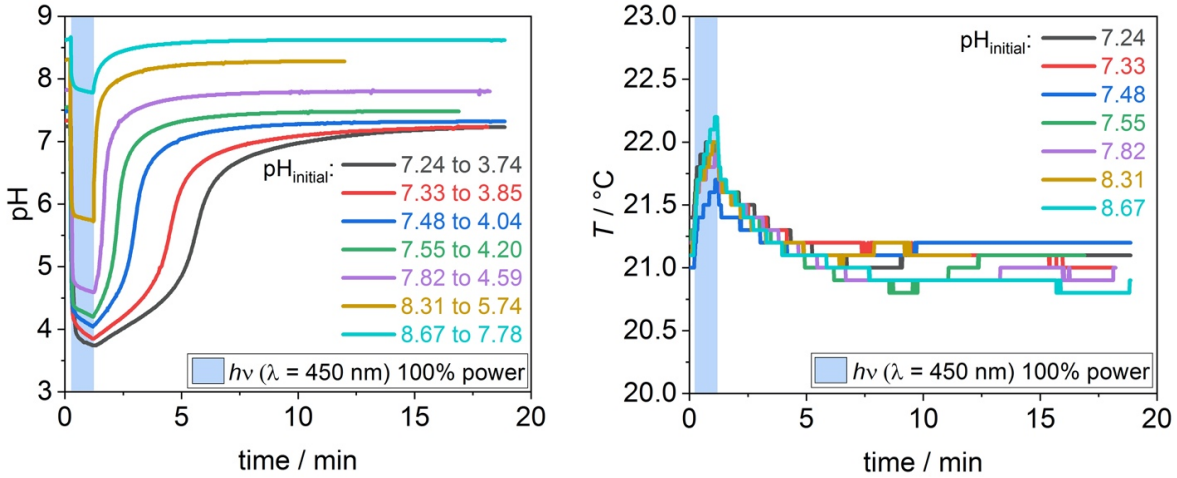


0.21 mM

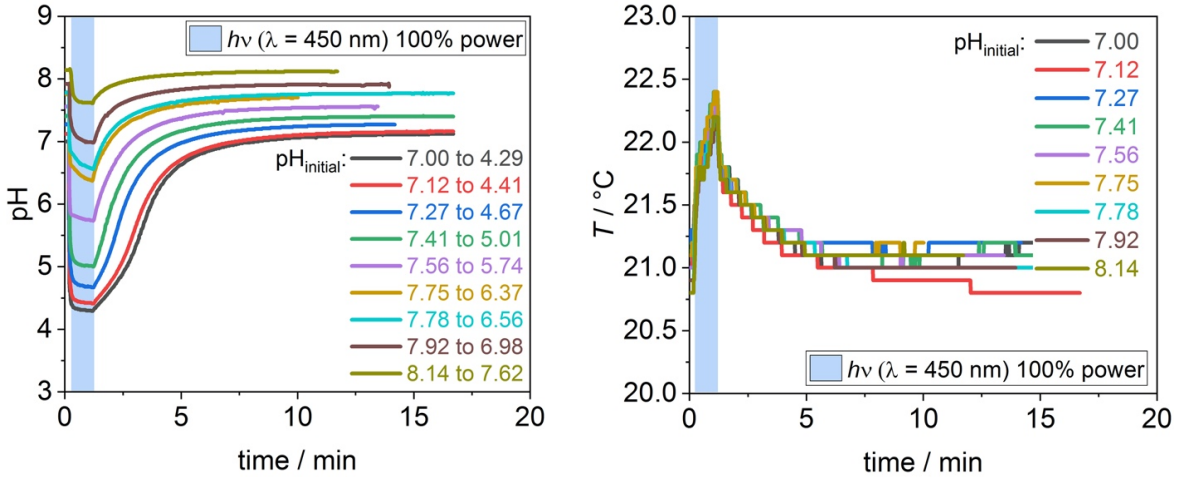


**Figure S14**. pH switching of a solution of **1** (2.4 mM, top and 0.21 mM bottom): pH trace over time at different initial pH values (left) and respective temperature profiles of measurements (right).

**Repeated pH switching cycles**

To measure the fatigue resistance of **1**: the initial pH with the maximum pH jump (pH ~ 7.2) and the highest initial pH with significant switching (pH ~ 8.3). We measure ten consecutive cycles by restarting the program of the photoreactor immediately after finishing. The first irradiation cycle followed by recovery of the pH is shown in Table S7 (top) as well as consecutive switching cycles (bottom). At both pH values we observed a high percentage of recovery per switching cycle (based on the pH).

**Table S7**. pH switching experiments of photoacid **1** in Penn PhD photoreactor. Experimental conditions: [**1**] = 3.0 mM in aqueous 20 mM KCl with addition of 0.7 µL (for pH ~ 7.2) or 7 µL (for pH ~ 8.3) of 1.0 M KOH respectively.

| | pH ~ 7.2 | pH ~ 8.3 |
|---|---|---|
| First cycle | 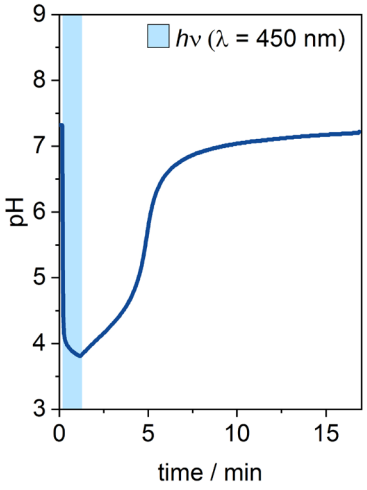 | 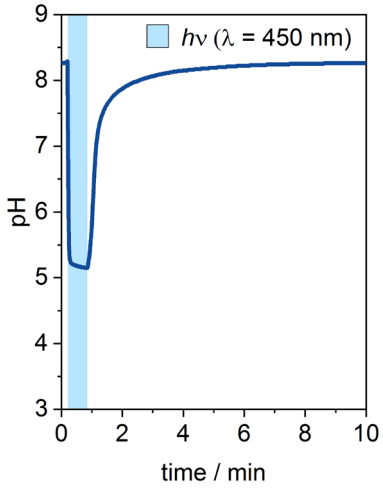 |
| 10 cycles | 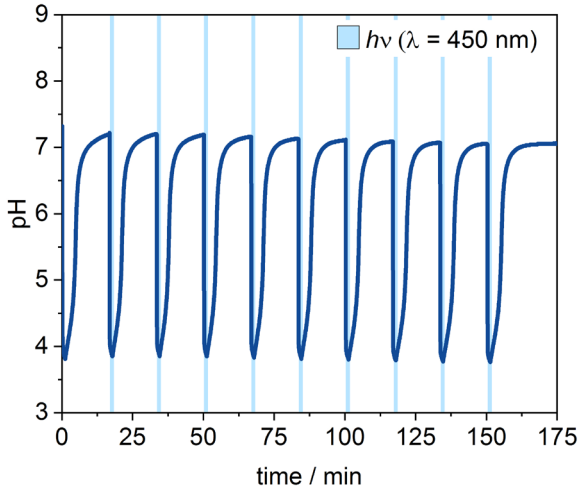 | 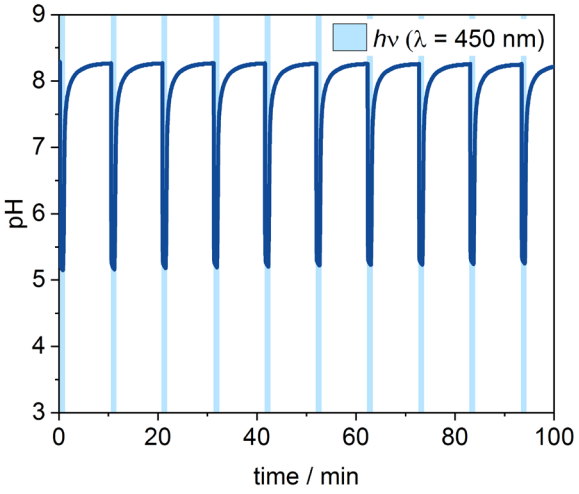 |
| Change in ΔpH from cycle #1 to final cycle | 3.51 to 3.29<br>98% recovery / cycle[a] | 3.12 to 3.00<br>99% recovery / cycle[a] |
| Temperature | 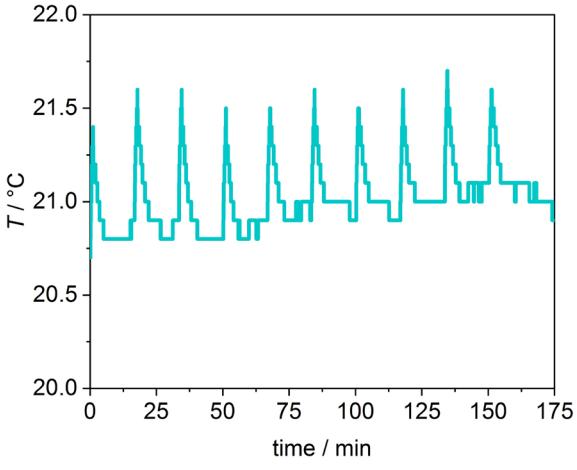 | 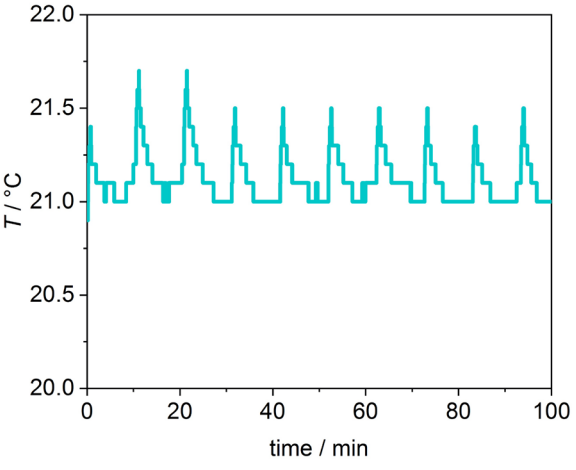 |

a) $\%recovery/cycle = \left(\frac{\Delta pH_{final\ cycle}}{\Delta pH_{first\ cycle}}\right)^{\frac{1}{\#\ of\ cycles}}$

## S5.2. Cary 60 LED setup

The light irradiation setup in the Cary60 UV-vis spectrometer (as described in section S4.2) was used to increase the number of pH switching cycles by automation. In addition to pH and temperature the change in absorbance of a dilute sample (0.3 mM) was monitored. Despite using the temperature control spikes in temperature during the irradiation time could not be avoided.

**Repeated pH switching cycles**

**Table S8**. Light induced (λ = 455 nm) pH switching of **1** in a 1 cm cuvette at 25°C: changes in pH, temperature, and absorbance of a dilute (0.3 mM) and concentrated (3 mM) sample monitored simultaneously. The pH and temperature were constant after the irradiation cycles.

| c / mM | 0.3 | 3 |
|---|---|---|
| # of cycles | 12 | 25 |
| pH | 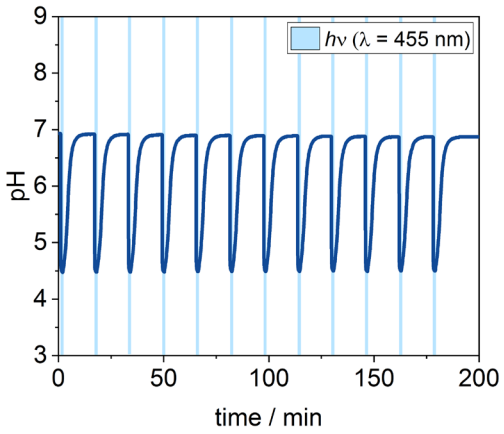 | 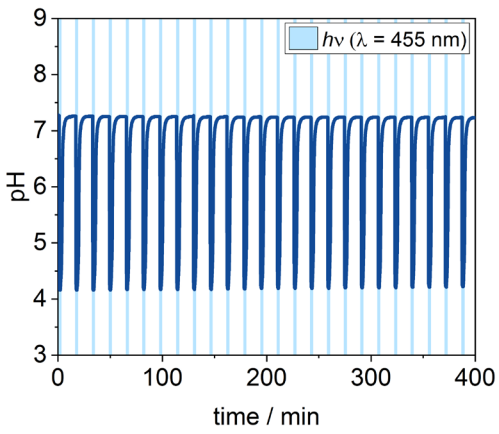 |
| Change in ΔpH | 2.45 to 2.37<br>99% recovery / cycle | 3.11 to 3.02<br>99% recovery / cycle |
| Temperature | 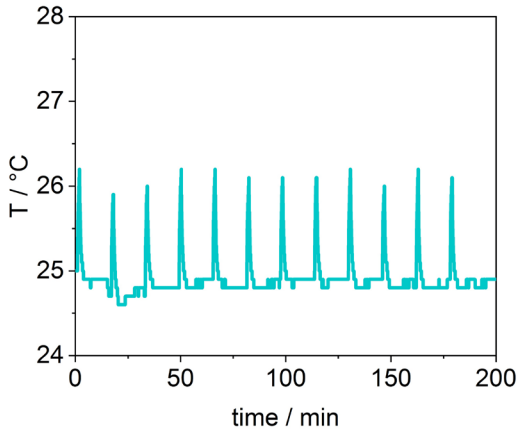 | 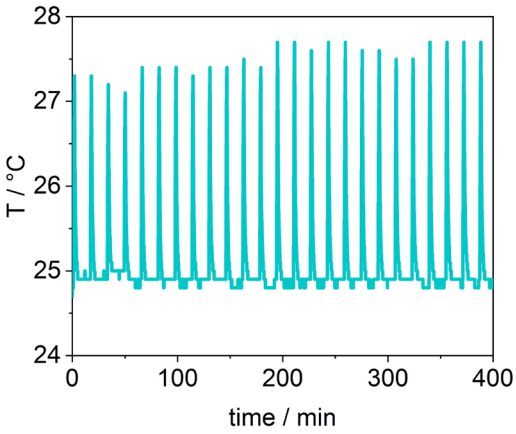 |
| Absorbance | 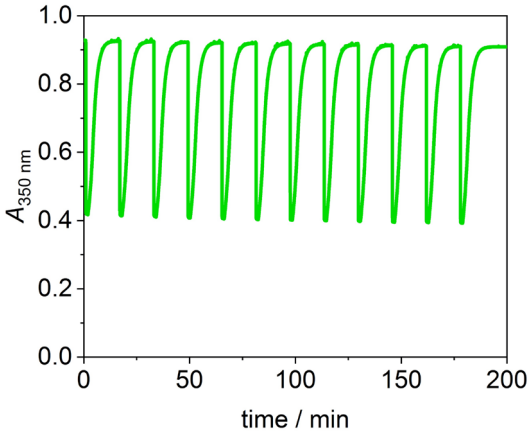 | Too optically dense to measure |

**Variable temperature**

The effect of temperature on the pH change and equilibrium position was investigated at 22°C, 25°C and 28°C (Figure S15) of a 0.3 mM solution of **1**. As to be expected the lowest temperature resulted in the slowest pH recovery after irradiation and the highest temperature resulted in the fastest pH recovery (18 *vs* 7 min). The equilibrium positions appear to be slightly shifted with the highest temperature having a lower equilibrium pH and the lowest temperature having the highest equilibrium pH. However, the equilibrium of the lowest and the highest temperature only differ by 0.05 pH units.

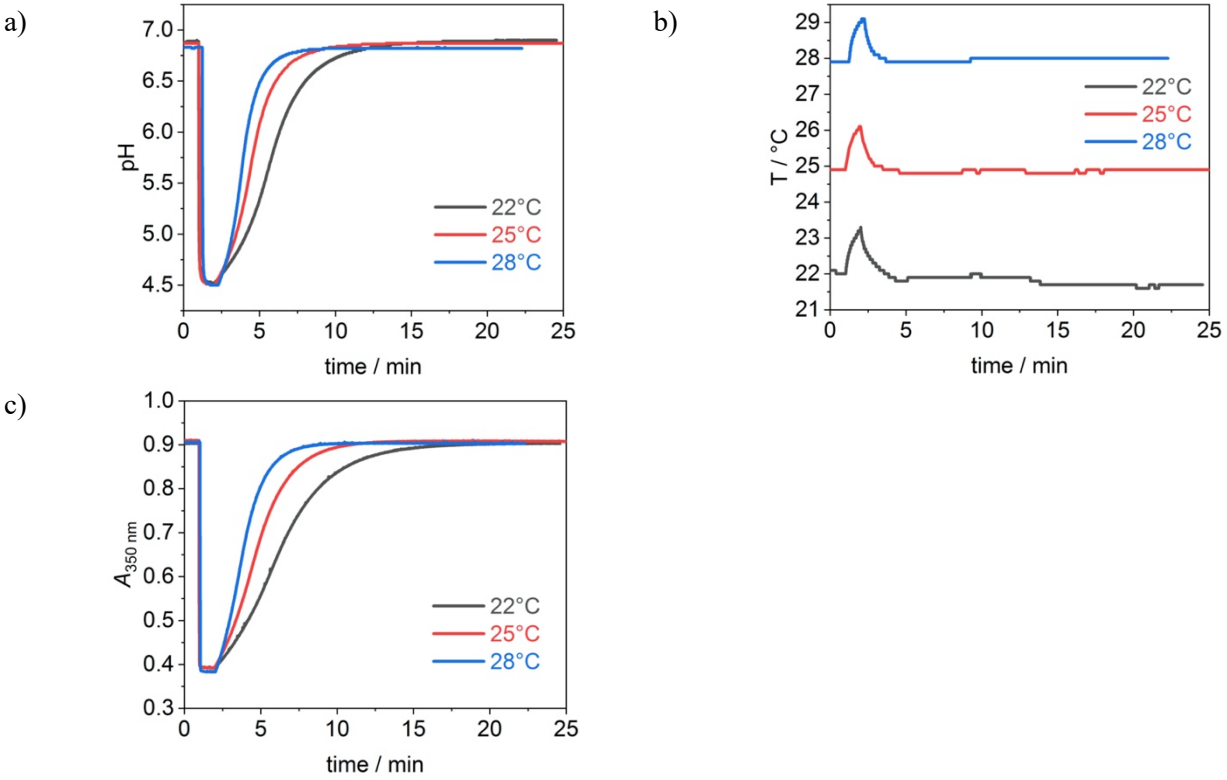


**Figure S15**. pH switching of a dilute sample of **1** (0.3 mM) at different temperatures in the Cary 60. a) pH change over time at 22, 25 and 28°C, b) Temperature change over time at initial temperatures of 22, 25 and 28°C, c) Change in absorbance at 350 nm over time at 22, 25 and 28°C.

## S6. Switching a pH indicator dye – bromothymol blue

We chose to control the protonation of bromothymol blue (BTB) with photoacid **1** as this indicator dye is used for a pH change from basic to acidic.

The change of absorbance of BTB from pH 4–9 is shown in Figure S16. Samples were prepared from 2.00 mL of stock solution of BTB in milliQ water (35.2 µM) and 1.00 mL of phosphate buffer (0.10 M) at respective pH values.

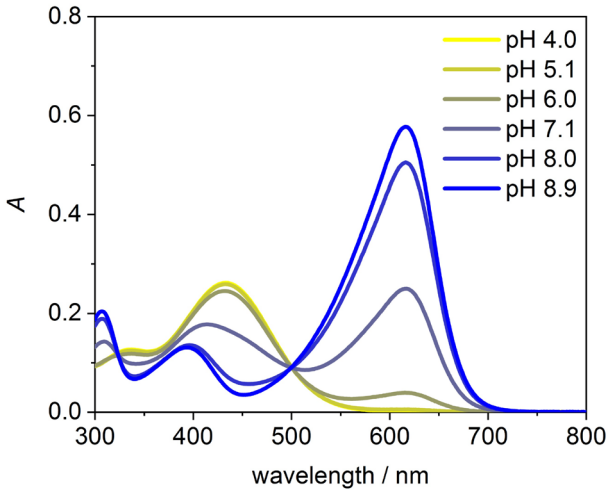


**Figure S16**. pH dependent absorbance spectra of bromothymol blue (23.5 µM, [phosphate] = 33 mM, $T$ = 20 °C).

Aqueous samples of **1** (1.2 mM) and a mixture of **1** (1.2 mM) with bromothymol blue (BTB, 0.17 mM) were prepared with milliQ water and the pH was adjusted to pH ~8 with 0.1–1 M aqueous potassium hydroxide. UV-vis absorption spectra were collected in a 1 mm × 1 mm quartz cuvette in a Cary60 instrument with a LED setup as described in S4.2. Samples were irradiated at $T$ = 22 °C with 450 nm light until a photostationary state was reached (Figure S17, yellow). The thermal recovery in the dark was monitored until no further absorbance changes could be observed (Figure S17, purple). The recovered spectra matched the initial spectra in the dark before irradiation.

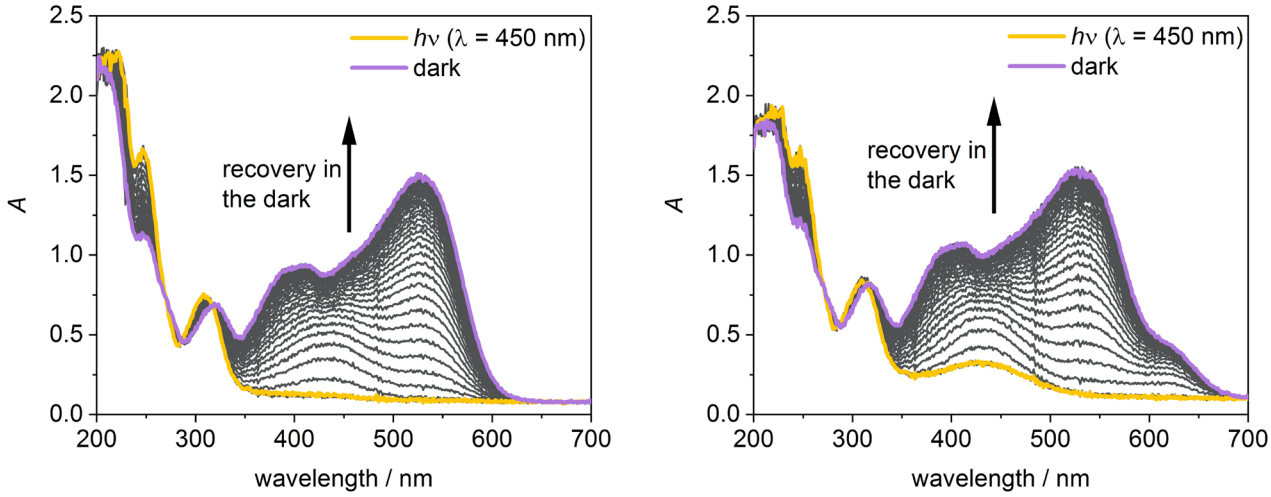


**Figure S17**. Absorbance spectra of **1** (1.2 mM, left) and a mixture of **1** (1.2 mM) and BTB (0.17 mM, right) showing the thermal recovery after reaching a photostationary state with λ = 450 nm light (yellow). The fully equilibrated absorbance trace in the dark is shown in purple. Scans were collected every 12 s.

Irradiation of an aqueous sample of **1** (1.2 mM) resulted in a complete bleach in the visible range confirming full conversion of the MC(H) to the SP form under irradiation (Figure S18, yellow dashed). The absorbance spectrum of a mixture of **1** (1.2 mM) and bromothymol blue (0.17 mM) at pH ~ 8 (Figure S18) shows the characteristic absorbance of **1** (purple) as well as the characteristic absorbance maximum of bromothymol blue at 615 nm (blue, see Fig S16 for pH dependent absorption spectra). Under irradiation with 450 nm light an absorbance maximum at 430 nm (Figure S18, orange) persisted in the visible range which was previously not visible for a solution of **1**. This maximum is characteristic for bromothymol blue at pH 5–6 (Figure S18, orange dashed) confirming a decrease in the pH value under irradiation. After irradiation the thermal recovery in the dark produced the initial absorption spectrum at equilibrium. The characteristic change in the absorbance of bromothymol blue confirms that it is possible to control the protonation state of a pH indicator dye used for basic to acidic pH ranges.

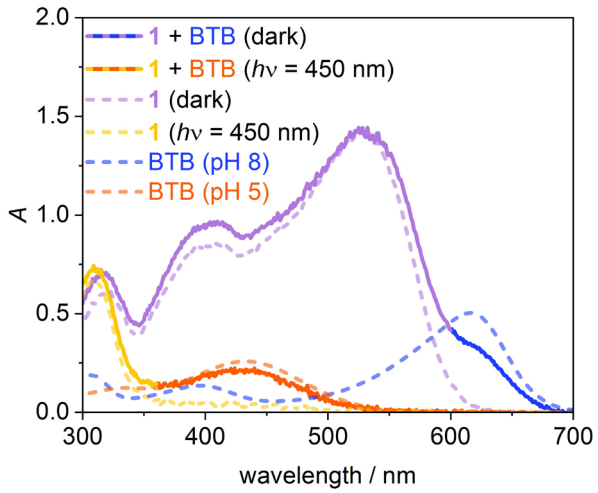


**Figure S18**. UV-vis absorbance spectra of **1** (purple dashed, yellow dashed) and a mixture of **1** + BTB (purple-blue, yellow-orange) in the dark and under 450 nm irradiation respectively as well as the pH dependent absorbance spectra of BTB at pH 8 (blue dashed) and at pH 5 (orange dashed).

Photographs of the aqueous solutions of **1** (1.2 mM) and a mixture of **1** (1.2 mM) with BTB (0.17 mM) are shown in Table S9. Samples are shown before irradiation (equilibrated in the dark) and after irradiation with λ = 450 nm. By using a 1 mm × 1 mm cuvette mixing of the samples could be minimised which enabled us to create localised pH minima using masks to control which portions of the sample are irradiated (Table S9, middle and right column).

**Table S9**. Photographs of an aqueous sample of **1** (1.2 mM) and a mixture of **1** (1.2 mM) with BTB (0.17 mM) before irradiation, after irradiation with λ = 450 nm and after irradiation to generate localized pH changes.

| | Equilibrated in the dark | After localized *hν* (λ = 450 nm), large area irradiated | After localized *hν* (λ = 450 nm), small areas irradiated with grid |
|---|---|---|---|
| **1** (1.2 mM) |  |  | 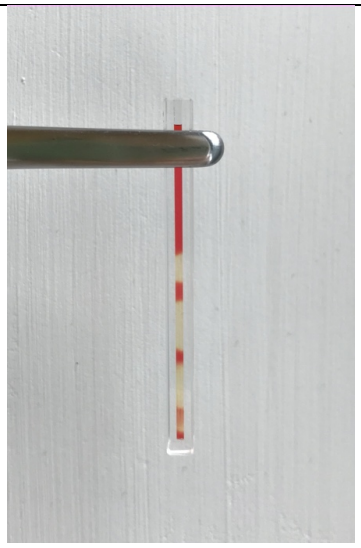 |
| **1** (1.2 mM) + BTB (0.17 mM) |  |  | 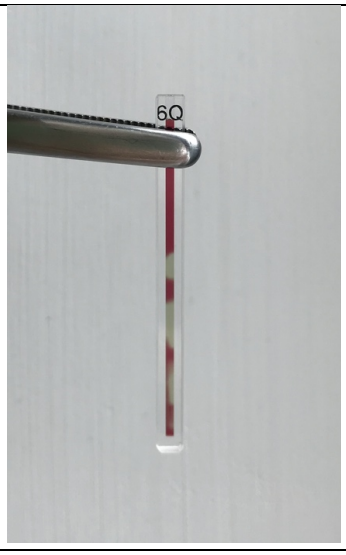 |

# S7. Bibliography


[1] N. Mallo, E. D. Foley, H. Iranmanesh, A. D. W. Kennedy, E. T. Luis, J. Ho, J. B. Harper, J. E. Beves, *Chem. Sci.* **2018**, *9*, 8242-8252.

[2] L. Wimberger, S. K. K. Prasad, M. D. Peeks, J. Andreasson, T. W. Schmidt, J. E. Beves, *J. Am. Chem. Soc.* **2021**, *143*, 20758-20768.

[3] C. Berton, D. M. Busiello, S. Zamuner, E. Solari, R. Scopelliti, F. Fadaei-Tirani, K. Severin, C. Pezzato, *Chem. Sci.* **2020**, *11*, 8457-8468.

[4] N. Mallo, P. T. Brown, H. Iranmanesh, T. S. C. MacDonald, M. J. Teusner, J. B. Harper, G. E. Ball, J. E. Beves, *Chem. Commun.* **2016**, *52*, 13576-13579.